Anomalous signature-dependence of rotational bands in odd-A nuclei explained in terms of γ vibration

Akitsu Ikeda* and Takafumi Shimano
Department of Physics, Tokyo Institute of Technology, Oh-okayama, Meguro, Tokyo 152, Japan
(Received 1 March 1990)

The anomalous signature-dependence of proton $h_{11/2}$ rotational bands in ^{155,157}Ho, ^{159}Tm, ^{161,163,165}Lu after the first band crossing is described in the framework of a model of particles plus symmetric rotor. We take into account rotor's degree of freedom that it undergoes γ vibration about an axially symmetric equilibrium deformation. By using a set of moments of inertia such that the largest one is around the shortest axis, the essential features of all the energy spectra are reproduced. We have calculated magnetic dipole and electric quadrupole transition strengths with the wave functions obtained, and have found that virtually every characteristic feature of the available experimental data is well reproduced.

I. INTRODUCTION

It was found in 1981 that the energy spectrum of the negative-parity yrast rotational band of ^{159}Tm is anomalous in its dependence on a quantum number called signature.[1-6] Since then the same kind of anomaly has been found in ^{155}Ho,[7] ^{157}Ho,[7-11] ^{161}Lu,[12] ^{163}Lu,[13] and ^{165}Lu.[14-17] This anomaly has long challenged us for an explanation. Recently we have proposed a model, in which the anomaly of ^{157}Ho has been well reproduced in a natural way.[18] In this paper we will extend numerical calculations to the other nuclei and compare the theoretical results with the experimental data. In order to test the validity of the model, magnetic dipole and electric quadrupole transition strengths will be calculated by using the wave functions obtained and the predictions will be compared with the available experimental data.

We will devote the present section to a brief description of the phenomenon of interest. Signature is a quantum number related to the invariance of a system with quadrupole deformation under its rotation by 180° around a principal axis. Thus we can call the symmetry turn-about invariance. When the system is axially symmetric, only the turn-about around principal axes other than the symmetry axis can be used to define the signature quantum number. Signature takes on only two different values in odd-A nuclei, according to the total spin. It is customary to assign

$$\alpha_I = \tfrac{1}{2}(-1)^{I-1/2} \tag{1.1}$$

as the signature quantum number to a state of spin I of an odd-A nucleus.

In Bohr and Mottelson's strong coupling model, a rotational band is characterized by its intrinsic structure and is a sequence of levels differing in spin by $1\hbar$. Signature now splits such a rotational band into two families, each consisting of levels differing in spin by $2\hbar$ according to Eq. (1.1).

The significance of signature is easier to see in the low-lying negative-parity rotational bands of the odd-A Ho, Tm, and Lu isotopes which we are interested in. The intrinsic structure of these bands is such that the last odd proton moves in the orbitals originating from $h_{11/2}$. They are called unique-parity orbitals because they are isolated in energy from other orbitals of the same parity and therefore are rather pure in j quantum number. To a good approximation we can assume that j is a good quantum number in these orbitals. Then, each of these bands is split into $I \equiv j$ (mod2) and $I \equiv j+1$ (mod2) families according to signature. It is observed that the energy spectrum and the reduced $M1$ transition probabilities of a unique-parity rotational band depend on signature in characteristic ways. The $I \equiv j$ (mod2) sequence is shifted downward in energy against the other. This is why the $I \equiv j$ (mod2) sequence is customarily called the favored band and the other, unfavored. $B(M1; I \to I-1)$'s are larger in many nuclei when the state I is a favored state than when it is an unfavored state. The simple model of a particle coupled to a symmetric rotor predicts such a dependence of energy spectra and $B(M1)$'s on signature as a consequence of the Coriolis coupling, in accordance with a great deal of experimental data. We will call such a dependence of energy spectra and $B(M1)$'s on signature normal signature dependence.

It is important to note that the signature quantum number is directly connected with the characteristic energy shift and alternating enhancement of $M1$ transitions and that these are well understood theoretically in terms of the simple particle-rotor model.

When we go up along such a negative-parity yrast band we come across a discontinuity, sharp or broad, in the energy versus spin diagram. The widely accepted interpretation of this discontinuity is that it results from the crossing of two bands. One of them is just the rotational band whose structure we have already discussed above. It should be noted that the angular momentum of the last odd quasiproton, which moves in the orbitals originating from $h_{11/2}$, aligns itself with the total angular momentum to some extent. In the other band two quasineutrons are excited in addition. They move in the orbitals originating from the spherical $i_{13/2}$ and align their spins with the to-

tal angular momentum. It may be appropriate to call the former band $(\pi h_{11/2})^1$ and the latter $(\pi h_{11/2})^1(\nu i_{13/2})^2$. Despite the difference between the configurations of the two bands, the particles plus symmetric rotor model predicts that the correspondence of the signature quantum number to energy favoredness or unfavoredness invariably persists.

To our surprise the opposite to this prediction is observed in ^{155,157}Ho, ^{159}Tm, and ^{161,163,165}Lu after the band crossing: the $I-j$=even levels are found to lie higher in energy than the $I-j$=odd levels where j stands for $h_{11/2}$. We illustrate the energy spectra of those isotopes in Fig. 1 in the form

$$\Theta_I \equiv \frac{E(I)-E(I-1)}{2I} , \tag{1.2}$$

where $E(I)$ is the energy of the state of spin I. In Fig. 1 black points are given to Θ_I's when I belongs to the favored band and open circles otherwise. The signature dependence is normal when the open circles are above the black points in the illustration. We see that the signature dependence is normal up to the band crossing and that it gets inverted after that for a rather wide range of spin. Since the signature inversion is rather subtle and hard to see, the spectra in the region of signature inversion are magnified in the insets. This anomaly constitutes the problem of signature inversion and seems to provide us with an opportunity to learn about unknown aspects of nuclear structure.

Through the introduction of an equilibrium triaxial deformation[19] or dynamical triaxial fluctuations around an equilibrium axially symmetric deformation[20] into the particle-rotor model we have learned that the triaxial degree of freedom influences the signature dependence of electromagnetic transition strengths. We have pursued the dynamical view of Ref. 20 and proposed a model for the signature inversion in a recent paper,[18] which is a straightforward extension of the model of Ref. 20. We applied the model to ^{157}Ho and reproduced its anomalous energy spectrum.

In this model the $(\pi h_{11/2})^1$ and $(\pi h_{11/2})^1(\nu i_{13/2})^2$ quasiparticle configurations are taken into consideration explicitly. In addition to them we let the rotor undergo γ-vibration around the equilibrium axially symmetric deformation.

In classical language, γ-vibration introduces time-dependent deviations of the system from axial symmetry and gives rise to two effects.

(1) It changes the mean field felt by quasiparticles leading to particle-vibration coupling.

(2) It allows the system to undergo three-dimensional rotation. This gives rise to rotation-vibration coupling.

The isotopes of interest are supposed to have axially symmetric deformations. The dependence of the moments of inertia on γ in the neighborhood of a prolate axially symmetric deformation is very crucial. We have found in Ref. 18 that the moments of inertia in the irrota-

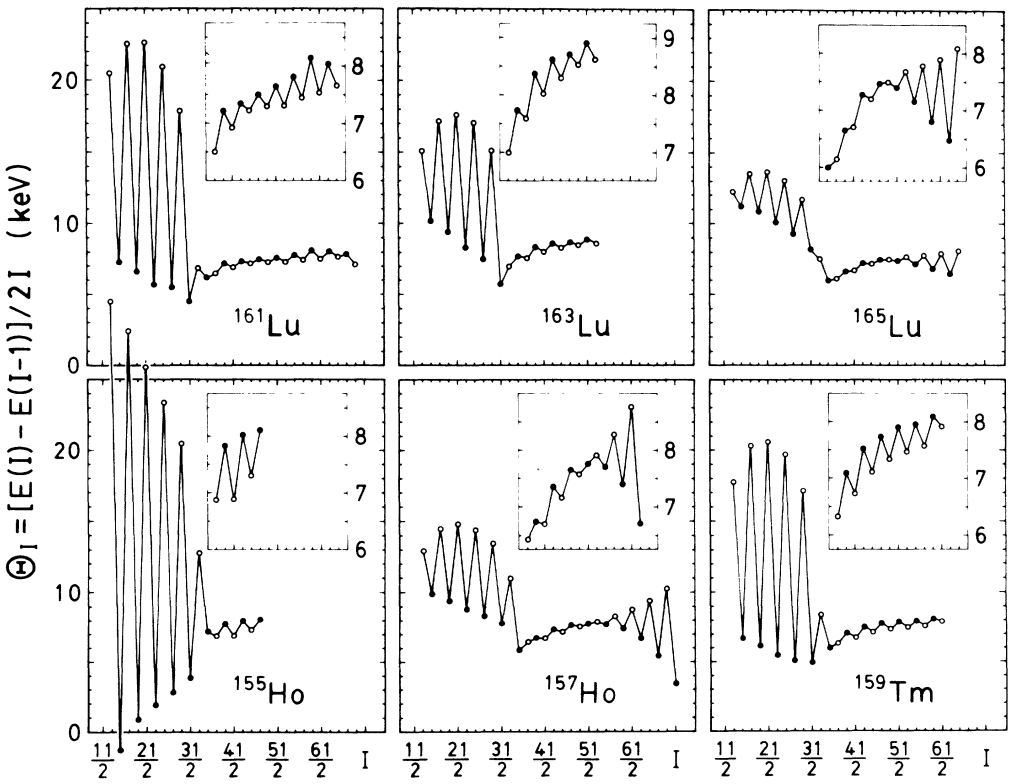

FIG. 1. Experimental energy spectra of ^{155,157}Ho, ^{159}Tm, and ^{161,163,165}Lu in the form of Θ_I, which is defined in Eq. (1.2). The black and white points correspond to I=favored and unfavored, respectively. Black points above white points mean signature inversion. A part of the spectra is illustrated with a four times larger scale in insets.

tional flow model (IRF) do not lead to an anomaly of the energy spectra. An important feature of the IRF moments of inertia is that the largest moment of inertia is around the axis of intermediate length. To reproduce the anomalous signature dependence we need a set of moments of inertia such that the largest and intermediate moments of inertia are around the shortest and intermediate axes, respectively. The longest axis is the symmetry axis when $\gamma=0°$ and the moment of inertia around the symmetry axis must be zero. Hence, the moment of inertia around the longest axis is expected to be proportional to γ^2 in the neighborhood of $\gamma=0°$. We will refer to this kind of moments of inertia as the Largest-around-Shortest (L-a-S) moments of inertia in this paper. This is the same feature that the classical rigid body moments of inertia have. It should be understood that presently we are not interested in the global behavior of the moments of inertia but only in their behavior in the neighborhood of a prolate axially symmetric deformation.

The model, which we know is able to reproduce the anomalous signature dependence of the energy spectrum of ^{157}Ho, should be tested further. First we will apply it to the above-mentioned Ho, Tm, and Lu isotopes to see whether or not the model is able to describe the anomaly in those isotopes. Then we will use the wave functions obtained to predict $M1$ and $E2$ transition probabilities. The predictions will be compared with experimental data when available. This is expected to provide a good way to test the model.

II. THE MODEL

A. Hamiltonian

The present model is a straightforward extension of the model of Ref. 20 to include not only one-quasiparticle configurations but also three-quasiparticle configurations. We write down the total Hamiltonian of the particles plus symmetric rotor model with the γ-vibrational degree of freedom as

$$H=H_{\text{particle}}+H_c+H_{\text{int}} . \tag{2.1}$$

The first term, H_{particle}, is separated into the energy for protons and neutrons in the unique-parity orbitals ($j_p=h_{11/2}$, $j_n=i_{13/2}$) and the effective interaction between them:

$$H_{\text{particle}}=H_p+H_n+H_{pn} . \tag{2.2}$$

The Hamiltonian for protons ($\tau=p$) and neutrons ($\tau=n$) is expressed as

$$H_\tau=\sum_\Omega(\epsilon_{j_\tau\Omega}-\lambda_\tau)c^\dagger_{j_\tau\Omega}c_{j_\tau\Omega} -\tfrac{1}{2}\Delta_\tau\sum_\Omega(c^\dagger_{\tilde{j}_\tau\Omega}c^\dagger_{j_\tau\Omega}+c_{j_\tau\Omega}c_{\tilde{j}_\tau\Omega}) , \quad \text{with } \tau=p,n , \tag{2.3}$$

where $c^\dagger$ and c are creation and annihilation operators, respectively, for particles of the indicated quantum numbers. We use the following phase convention for time reversal:

$$c^\dagger_{\tilde{j}\Omega}=(-1)^{j+\Omega}c^\dagger_{j,-\Omega} . \tag{2.4}$$

In Eq. (2.3), λ_τ stands for the Fermi energy and Δ_τ for the pairing energy gap. Using the Bogoljubov transformation

$$c^\dagger_{j\Omega}=u_{j\Omega}\alpha^\dagger_{j\Omega}-v_{j\Omega}\alpha_{\tilde{j}\Omega} \quad (u_{j\Omega},v_{j\Omega}\geq 0) , \tag{2.5}$$

we express H_p+H_n in a diagonal form with respect to the quasiparticle operators $\alpha^\dagger$ and α:

$$H_{\text{q.p.}}=\sum_{\tau=p,n}\sum_\Omega\sqrt{(\epsilon_{j_\tau\Omega}-\lambda_\tau)^2+\Delta_\tau^2}\,\alpha^\dagger_{j_\tau\Omega}\alpha_{j_\tau\Omega} . \tag{2.6}$$

The Nilsson energies in Eq. (2.3) are given to a good approximation as

$$\epsilon_{j_\tau\Omega}=q_\tau\beta\langle j_\tau\Omega|Y_{2,0}|j_\tau\Omega\rangle =-\frac{1}{8}\left[\frac{5}{\pi}\right]^{1/2}q_\tau\beta\frac{3\Omega^2-j_\tau(j_\tau+1)}{j_\tau(j_\tau+1)} \quad (\tau=p,n) , \tag{2.7}$$

where

$$q_\tau=-\hbar\omega_0(N_\tau+\tfrac{3}{2}) , \tag{2.8a}$$

with

$$\hbar\omega_0=\hbar\mathring{\omega}_0(1-\tfrac{4}{3}\delta^2-\tfrac{16}{27}\delta^3)^{-1/6} \tag{2.8b}$$

and

$$\hbar\mathring{\omega}_0=41\,A^{-1/3}\ \text{MeV}, \quad \delta=\frac{3}{4}\left[\frac{5}{\pi}\right]^{1/2}\beta . \tag{2.8c}$$

In Eq. (2.8a), $N_p=5$ and $N_n=6$ for the rotational levels under study.

H_{pn} in Eq. (2.2) represents the effective interaction between proton and neutron:

$$H_{pn}=\sum_{\mu\nu\xi\eta}\langle j_p\mu,j_n\nu|V_{pn}|j_p\xi,j_n\eta\rangle:c^\dagger_{j_p\mu}c^\dagger_{j_n\nu}c_{j_n\eta}c_{j_p\xi}: , \tag{2.9}$$

where : : denotes the normal product with respect to the quasiparticle vacuum. As for the effective proton-neutron force we adopt the quadrupole-quadrupole force

$$V_{pn}=-\chi\sum_{\mu=-2}^{2}(-1)^\mu r_p^2Y_{2,\mu}(\theta_p,\phi_p)r_n^2Y_{2,-\mu}(\theta_n,\phi_n) . \tag{2.10}$$

The second term in Eq. (2.1) is the sum of the rotational energy and the kinetic (T_γ) and potential energies of γ-vibration of the rotor:

$$H_c=\sum_{\kappa=1}^{3}\frac{\hbar^2}{2\mathcal{J}_\kappa}(I_\kappa-J_\kappa)^2+T_\gamma+\tfrac{1}{2}C_\gamma\gamma^2 , \tag{2.11}$$

where $J_\kappa=j_{p\kappa}+j_{n\kappa}$. In the present model we start with the general form of moments of inertia which were given by Belyaev for quadrupole deformations:[21]

$$\mathcal{J}_\kappa=4\beta^2(B_0-B_1\cos\gamma_\kappa-B_2\cos2\gamma_\kappa)\sin^2\gamma_\kappa , \tag{2.12}$$

where $\gamma_\kappa=\gamma-\frac{2}{3}\pi\kappa(\kappa=1,2,3)$. In this expression, B_0, B_1, and B_2 can be any function of the invariants β^2 and $\beta^3\cos3\gamma$. In this study we assume these factors to be constants for simplicity.

Expanding the moments of inertia around $\gamma=0°$ and keeping only the lowest and second lowest order terms in γ, we obtain

$$\mathcal{J}_1=\mathcal{J}\left[1+\frac{2}{\sqrt{3}}a_\gamma\gamma+O(\gamma^2)\right], \tag{2.13a}$$

$$\mathcal{J}_2=\mathcal{J}\left[1-\frac{2}{\sqrt{3}}a_\gamma\gamma+O(\gamma^2)\right], \tag{2.13b}$$

$$\mathcal{J}_3=\tfrac{4}{3}\mathcal{J}'\gamma^2+O(\gamma^4), \tag{2.13c}$$

where

$$\mathcal{J}=3\beta^2(B_0+\tfrac{1}{2}B_1+\tfrac{1}{2}B_2), \tag{2.14}$$

$$\mathcal{J}'=3\beta^2(B_0-B_1-B_2), \tag{2.15}$$

$$a_\gamma=(B_0-\tfrac{1}{4}B_1+2B_2)/(B_0+\tfrac{1}{2}B_1+\tfrac{1}{2}B_2). \tag{2.16}$$

The choice of $B_0=$const and $B_1=B_2=0$ corresponds to the IRF moments of inertia and leads to $a_\gamma=1$. On the other hand an appropriate choice of B_0, B_1, and B_2 gives a negative value to a_γ, which is a characteristic of the L-a-S moments of inertia. We assume $a_\gamma=-1$ in our study. This value of a_γ corresponds to $B_0+\frac{1}{8}B_1+\frac{5}{4}B_2=0$.

Using the moments of inertia of Eqs. (2.13) we can write the rotational energy as

$$\sum_{\kappa=1}^{2}\frac{\hbar^2}{2\mathcal{J}_\kappa}(I_\kappa-J_\kappa)^2\approx H_{\rm rot}+H_{\text{rot-vib}}, \tag{2.17}$$

where

$$H_{\rm rot}\equiv\frac{\hbar^2}{2\mathcal{J}}(\mathbf{I}^2-I_3^2)-\frac{\hbar^2}{2\mathcal{J}}(I_+J_-+I_-J_+)+\frac{\hbar^2}{4\mathcal{J}}(J_+J_-+J_-J_+), \tag{2.18}$$

$$H_{\text{rot-vib}}\equiv-\frac{a_\gamma}{\sqrt{3}}\frac{\hbar^2}{2\mathcal{J}}\gamma[(I_+^2+I_-^2)-2(I_+J_++I_-J_-)+(J_+^2+J_-^2)]. \tag{2.19}$$

Following Eq. (9.25) of Ref. 21 we express the kinetic energy of γ-vibration for small γ's,

$$T_\gamma\approx-\frac{\hbar^2}{2\beta^2B'_\gamma}\frac{1}{\gamma}\frac{\partial}{\partial\gamma}\left[\gamma\frac{\partial}{\partial\gamma}\right], \tag{2.20}$$

where

$$B'_\gamma=B_0-B_2-B_1\cos3\gamma\approx\frac{\mathcal{J}'}{3\beta^2}+O(\gamma^2). \tag{2.21}$$

Thus we have constructed an approximate Hamiltonian for γ-vibration as

$$H_{\rm vib}=-\frac{\hbar^2}{2\beta^2B_\gamma}\frac{1}{\gamma}\frac{\partial}{\partial\gamma}\left[\gamma\frac{\partial}{\partial\gamma}\right]+\frac{\hbar^2}{8\beta^2B_\gamma}\frac{1}{\gamma^2}(I_3-J_3)^2+\tfrac{1}{2}C_\gamma\gamma^2, \tag{2.22}$$

where B_γ means $B'_\gamma(\gamma=0°)$ of Eq. (2.21). In Eq. (2.22) we replace $I_3-J_3\equiv R_3$ with eigenvalues Λ ($\Lambda=0,\pm2,\pm4,\ldots$). Then the wave functions of γ-vibration are solutions of

$$H_{\rm vib}\psi_{\Lambda n}(\gamma)=E^\gamma_{\Lambda n}\psi_{\Lambda n}(\gamma). \tag{2.23}$$

Their eigenvalues are obtained to be

$$E^\gamma_{\Lambda n}=(2n+\tfrac{1}{2}|\Lambda|+1)E_\gamma\quad(n=0,1,2,\ldots), \tag{2.24}$$

where

$$E_\gamma=\frac{\hbar}{|\beta|}\left[\frac{C_\gamma}{B_\gamma}\right]^{1/2}. \tag{2.25}$$

We define the matrix element of γ between the vacuum and the γ-vibrational state as

$$b\equiv\langle\Lambda=2,n=0|\gamma|\Lambda=0,n=0\rangle=\int_{-\infty}^{\infty}\psi_{20}(\gamma)\gamma\psi_{00}(\gamma)|\gamma|d\gamma, \tag{2.26}$$

where we assume $\psi_{\Lambda n}(\gamma)$'s are normalized. Then we obtain

$$b^2=\frac{\hbar}{|\beta|\sqrt{B_\gamma C_\gamma}}. \tag{2.27}$$

Once we assign definite values to the parameters β, $\mathcal{J}$, E_γ, b^2, and a_γ, then B_0, B_1, and B_2 of Eq. (2.12) are determined uniquely. In Appendix B we give explicit expressions of B_0, B_1, and B_2 in terms of the parameters.

The third term in Eq. (2.1) represents the particle-vibration coupling:

$$H_{\rm int}=H_{p\text{-vib}}+H_{n\text{-vib}}, \tag{2.28}$$

where

$$H_{\tau\text{-vib}}=q_\tau\beta\left[(\cos\gamma-1)\sum_\Omega\langle j_\tau\Omega|Y_{2,0}|j_\tau\Omega\rangle c^\dagger_{j_\tau\Omega}c_{j_\tau\Omega}+\frac{1}{\sqrt{2}}\sin\gamma\sum_{\Omega'\Omega}\langle j_\tau\Omega'|Y_{2,2}+Y_{2,-2}|j_\tau\Omega\rangle c^\dagger_{j_\tau\Omega'}c_{j_\tau\Omega}\right]$$
$$\approx\frac{1}{\sqrt{2}}q_\tau\beta\gamma\sum_{\Omega'\Omega}\langle j_\tau\Omega'|Y_{2,2}+Y_{2,-2}|j_\tau\Omega\rangle c^\dagger_{j_\tau\Omega'}c_{j_\tau\Omega},\quad\text{with }\tau=p,n. \tag{2.29}$$

Summing up the partial Hamiltonian described above, the total Hamiltonian is written as

$$H = H_{\text{q.p.}} + H_{\text{rot}} + H_{\gamma} + H_{\text{pn}} \ , \tag{2.30}$$

where H_{γ} represents the sum of all the γ-dependent terms:

$$H_{\gamma} = H_{\text{vib}} + H_{\text{rot-vib}} + H_{p\text{-vib}} + H_{n\text{-vib}} \ . \tag{2.31}$$

Explicit forms of the Hamiltonian matrix elements are given in Appendix A.

B. Model space

The basis functions consist of one-quasiproton states with the γ-vibrational degree of freedom:

$$|\Psi^{IMK}_{\rho,\Lambda n}\rangle = \left[\frac{2I+1}{16\pi^2}\right]^{1/2} [\mathcal{D}^I_{MK}(\omega)\psi_{\Lambda n}(\gamma)\alpha^{\dagger}_{j_p\rho}|0\rangle + (-1)^{I-j_p}\mathcal{D}^I_{M,-K}(\omega)\psi_{-\Lambda,n}(\gamma)\alpha^{\dagger}_{j_p,-\rho}|0\rangle] \quad (K=\rho+\Lambda>0) \ , \tag{2.32}$$

and one-quasiproton and two-quasineutron states with the γ-vibrational degree of freedom

$$|\Psi^{IMK}_{\rho,\sigma\tau,\Lambda n}\rangle = \left[\frac{2I+1}{16\pi^2}\right]^{1/2} [\mathcal{D}^I_{MK}(\omega)\psi_{\Lambda n}(\gamma)\alpha^{\dagger}_{j_p\rho}\alpha^{\dagger}_{j_n\sigma}\alpha^{\dagger}_{j_n\tau}|0\rangle + (-1)^{I+j_p}\mathcal{D}^I_{M,-K}(\omega)\psi_{-\Lambda,n}(\gamma)\alpha^{\dagger}_{j_p,-\rho}\alpha^{\dagger}_{j_n,-\sigma}\alpha^{\dagger}_{j_n,-\tau}|0\rangle]$$

$$(K=\rho+\sigma+\tau+\Lambda>0, \ \sigma>\tau) \ , \tag{2.33}$$

where ρ, σ, τ, and Λ denote the projection of the spins of quasiparticles and γ-vibration on the symmetry axis of the rotor. In the present model we take into account the vacuum ($\Lambda=n=0$), and the state of one γ-vibrational quantum ($\Lambda=\pm2$, $n=0$).

When we work in the space of two-quasineutron configurations of the BCS approximation, the spurious states related to violation of particle number conservation inevitably creeps in. The spurious states are of one-quasiproton and two-quasineutron configurations and can be written as

$$(\hat{N}_n - \langle 0|\hat{N}_n|0\rangle)|\Psi^{IMK}_{\rho,\Lambda n}\rangle \ , \tag{2.34}$$

where $\hat{N}_n$ is the number operator for $i_{13/2}$ neutrons. We have rigorously eliminated them out of the basis functions in this study.

C. Magnetic dipole transitions

The $M1$ operator in the laboratory system assumes the form

$$\mathcal{M}_{\mu}(M1) = \sum_{\nu=-1}^{1} \mathcal{D}^1_{\mu\nu}(\omega)\mathcal{M}'_{\nu}(M1) \ , \tag{2.35}$$

where $\mathcal{M}'_{\mu}(M1)$ is the $M1$ operator in the intrinsic system:

$$\mathcal{M}'_{\mu}(M1) = \mu_N \left[\frac{3}{4\pi}\right]^{1/2} [g_R I_{\mu} + (g_{j_p} - g_R)j_{p\mu} + (g_{j_n} - g_R)j_{n\mu}] \ , \tag{2.36}$$

where μ_N is the nuclear magneton. In terms of the spin and orbital g factors we write the g factors of quasiparticles in unique-parity orbitals as

$$g_{j_\tau} = \frac{1}{2j_\tau(j_\tau+1)}\{[j_\tau(j_\tau+1) - l_\tau(l_\tau+1) + \tfrac{3}{4}]g_s(\tau) + [j_\tau(j_\tau+1) + l_\tau(l_\tau+1) - \tfrac{3}{4}]g_l(\tau)\}, \quad \text{with } \tau = p,n \ . \tag{2.37}$$

In the present study we assume $g_R = Z/A$ for the rotor and the bare values for g_s and g_l.

Matrix elements of the $M1$ operator are reduced to the expressions

$$\begin{aligned}\langle \Psi^{I'K'}_{\rho',\Lambda'n'} \| \mathcal{M}(M1) \| \Psi^{IK}_{\rho,\Lambda n}\rangle = \mu_N &\left[\frac{3}{4\pi}(2I+1)\right]^{1/2} \delta_{n'n} \\ &\times \Bigg[\delta_{I'I}\delta_{K'K}\delta_{\rho'\rho}\delta_{\Lambda'\Lambda} g_R \sqrt{I(I+1)} \\ &+ (g_{j_p} - g_R) \Bigg[\delta_{\Lambda'\Lambda} \sum_{\nu=-1}^{1} \delta_{K',K+\nu}\delta_{\rho',\rho+\nu}(IK1\nu|I'K+\nu)\langle 0|\alpha_{j_p,\rho+\nu} j_{p\nu}\alpha^{\dagger}_{j_p\rho}|0\rangle \\ &+ (-1)^{I'-j_p}\delta_{K'K}\delta_{K,1/2}\delta_{\rho',-\rho+1}\delta_{\Lambda',-\Lambda}(I\tfrac{1}{2}\,1-1|I'-\tfrac{1}{2}) \\ &\times \langle 0|\alpha_{j_p,\rho-1} j_{p,-1}\alpha^{\dagger}_{j_p\rho}|0\rangle \Bigg] \Bigg] \ ,\end{aligned} \tag{2.38a}$$

$$\langle \Psi^{I'K'}_{\rho',\Lambda'n'} \| \mathcal{M}(M1) \| \Psi^{IK}_{\rho,\sigma\tau,\Lambda n} \rangle = \mu_N \left[\frac{3}{4\pi}(2I+1) \right]^{1/2} (g_{j_n} - g_R)\delta_{n'n}$$
$$\times \left[\delta_{\rho'\rho}\delta_{\Lambda'\Lambda} \sum_{\nu=\pm 1} \delta_{K',K+\nu}\delta_{\sigma+\tau,-\nu}(IK1\nu|I'K+\nu)\langle 0|j_{n\nu}\alpha^{\dagger}_{j_n\sigma}\alpha^{\dagger}_{j_n,-\sigma-\nu}|0\rangle \right.$$
$$\left. + (-1)^{I'-j_p}\delta_{K'K}\delta_{K,1/2}\delta_{\rho',-\rho}\delta_{\sigma+\tau,1}\delta_{\Lambda',-\Lambda}(I\tfrac{1}{2}1-1|I'-\tfrac{1}{2})\langle 0|j_{n,-1}\alpha^{\dagger}_{j_n\sigma}\alpha^{\dagger}_{j_n,-\sigma+1}|0\rangle \right] , \tag{2.38b}$$

$$\langle \Psi^{I'K'}_{\rho',\sigma'\tau',\Lambda'n'} \| \mathcal{M}(M1) \| \Psi^{IK}_{\rho,\sigma\tau,\Lambda n} \rangle = \mu_N \left[\frac{3}{4\pi}(2I+1) \right]^{1/2} \delta_{n'n}$$
$$\times \left[\delta_{I'I}\delta_{K'K}\delta_{\rho'\rho}\delta_{\sigma'\sigma}\delta_{\tau'\tau}\delta_{\Lambda'\Lambda} g_R \sqrt{I(I+1)} \right.$$
$$+ (g_{j_p} - g_R) \left[\delta_{\sigma'\sigma}\delta_{\tau'\tau}\delta_{\Lambda'\Lambda} \sum_{\nu=-1}^{1} \delta_{K',K+\nu}\delta_{\rho',\rho+\nu}(IK1\nu|I'K+\nu)\langle 0|\alpha_{j_p,\rho+\nu}j_{p\nu}\alpha^{\dagger}_{j_p\rho}|0\rangle \right.$$
$$+ (-1)^{I'-j_p}\delta_{K'K}\delta_{K,1/2}\delta_{\rho',-\rho+1}\delta_{\sigma',-\tau}\delta_{\tau',-\sigma}\delta_{\Lambda',-\Lambda}(I\tfrac{1}{2}1-1|I'-\tfrac{1}{2})$$
$$\left. \times \langle 0|\alpha_{j_p,\rho-1}j_{p,-1}\alpha^{\dagger}_{j_p\rho}|0\rangle \right]$$
$$+ (g_{j_n} - g_R) \left[\delta_{\rho'\rho}\delta_{\Lambda'\Lambda} \sum_{\nu=-1}^{1} \delta_{K',K+\nu}(IK1\nu|I'K+\nu) \right.$$
$$\times (\delta_{\sigma',\sigma+\nu}\delta_{\tau'\tau}\langle 0|\alpha_{j_n,\sigma+\nu}j_{n\nu}\alpha^{\dagger}_{j_n\sigma}|0\rangle + \delta_{\sigma'\sigma}\delta_{\tau',\tau+\nu}\langle 0|\alpha_{j_n,\tau+\nu}j_{n\nu}\alpha^{\dagger}_{j_n\tau}|0\rangle)$$
$$+ (-1)^{I'-j_p}\delta_{K'K}\delta_{K,1/2}\delta_{\rho',-\rho}\delta_{\Lambda',-\Lambda}(I\tfrac{1}{2}1-1|I'-\tfrac{1}{2})$$
$$\times (\delta_{\sigma',-\tau}\delta_{\tau',-\sigma+1}\langle 0|\alpha_{j_n,\sigma-1}j_{n,-1}\alpha^{\dagger}_{j_n\sigma}|0\rangle$$
$$\left. \left. + \delta_{\sigma',-\tau+1}\delta_{\tau',-\sigma}\langle 0|\alpha_{j_n,\tau-1}j_{n,-1}\alpha^{\dagger}_{j_n\tau}|0\rangle) \right) \right] , \tag{2.38c}$$

where

$$\langle 0|\alpha_{j_\tau\mu}j_{\tau 0}\alpha^{\dagger}_{j_\tau\mu}|0\rangle = \mu \quad (\tau = p,n) , \tag{2.39a}$$

$$\langle 0|\alpha_{j_\tau,\mu\pm1}j_{\tau,\pm1}\alpha^{\dagger}_{j_\tau\mu}|0\rangle = \mp\frac{1}{\sqrt{2}}(u_{j_\tau\mu}u_{j_\tau,\mu\pm1} + v_{j_\tau\mu}v_{j_\tau,\mu\pm1})\sqrt{j_\tau(j_\tau+1)-\mu(\mu\pm1)} \quad (\tau = p,n) , \tag{2.39b}$$

$$\langle 0|j_{n,\pm1}\alpha^{\dagger}_{j_n\sigma}\alpha^{\dagger}_{j_n,-\sigma\mp1}|0\rangle = \pm\frac{1}{\sqrt{2}}(-1)^{j_n-\sigma}(u_{j_n\sigma}v_{j_n,\sigma\pm1} - v_{j_n\sigma}u_{j_n,\sigma\pm1})\sqrt{j_n(j_n+1)-\sigma(\sigma\pm1)} . \tag{2.40}$$

D. Electric quadrupole transitions

We can write the $E2$ operator as

$$\mathcal{M}_\mu(E2) = e_c\beta \left[\cos\gamma \mathcal{D}^2_{\mu0}(\omega) + \frac{1}{\sqrt{2}}\sin\gamma[\mathcal{D}^2_{\mu2}(\omega) + \mathcal{D}^2_{\mu,-2}(\omega)] \right] \approx e_c\beta \left[\mathcal{D}^2_{\mu0}(\omega) + \frac{1}{\sqrt{2}}\gamma[\mathcal{D}^2_{\mu2}(\omega) + \mathcal{D}^2_{\mu,-2}(\omega)] \right] , \tag{2.41}$$

where the effective charge of the rotor e_c is assumed to be

$$e_c = \frac{3}{4\pi}eZR_0^2 , \tag{2.42}$$

with

$$R_0 = 1.2A^{1/3} \text{ fm} . \tag{2.43}$$

In this expression it is assumed that the rotor has a uniform charge distribution. In Eq. (2.41) we have ignored the contribution from the quasiparticles. This is a reasonable approximation because the $E2$ transition in the isotopes of interest are dominated by the contribution from the collective rotation.

Matrix elements of the $E2$ operator are of the following forms:

$$\langle \Psi^{I'K'}_{\rho',\Lambda'n'} \| \mathcal{M}(E2) \| \Psi^{IK}_{\rho,\Lambda n} \rangle = e_c \beta \sqrt{2I+1} \times \left[\delta_{\rho'\rho} \left[\delta_{K'K} \delta_{\Lambda'\Lambda} \delta_{n'n} (IK20|I'K) + \frac{1}{\sqrt{2}} \sum_{\nu=\pm 2} \delta_{K',K+\nu} \delta_{\Lambda',\Lambda+\nu} \langle \Lambda+\nu, n'|\gamma|\Lambda n \rangle (IK2\nu|I'K+\nu) \right] + \frac{1}{\sqrt{2}} (-1)^{I'-j_p} \delta_{K',-K+2} \delta_{\rho',-\rho} \delta_{\Lambda',-\Lambda+2} \langle \Lambda-2, n'|\gamma|\Lambda n \rangle (IK2-2|I'K-2) \right] , \quad (2.44a)$$

$$\langle \Psi^{I'K'}_{\rho',\Lambda'n'} \| \mathcal{M}(E2) \| \Psi^{IK}_{\rho,\sigma\tau,\Lambda n} \rangle = 0 , \quad (2.44b)$$

$$\langle \Psi^{I'K'}_{\rho',\sigma'\tau',\Lambda'n'} \| \mathcal{M}(E2) \| \Psi^{IK}_{\rho,\sigma\tau,\Lambda n} \rangle = e_c \beta \sqrt{2I+1} \times \left[\delta_{\rho'\rho} \delta_{\sigma'\sigma} \delta_{\tau'\tau} \left[\delta_{K'K} \delta_{\Lambda'\Lambda} \delta_{n'n} (IK20|I'K) + \frac{1}{\sqrt{2}} \sum_{\nu=\pm 2} \delta_{K',K+\nu} \delta_{\Lambda',\Lambda+\nu} \langle \Lambda+\nu, n'|\gamma|\Lambda n \rangle (IK2\nu|I'K+\nu) \right] + \frac{1}{\sqrt{2}} (-1)^{I'-j_p} \delta_{K',-K+2} \delta_{\rho',-\rho} \delta_{\sigma',-\tau} \delta_{\tau',-\sigma} \delta_{\Lambda',-\Lambda+2} \langle \Lambda-2, n'|\gamma|\Lambda n \rangle \times (IK2-2|I'K-2) \right] . \quad (2.44c)$$

III. NUMERICAL RESULTS AND DISCUSSION

A. General

We first summarize the parameters involved and describe how we fix them. The parameters involved are axially symmetric equilibrium deformation β, Fermi energies λ_p and λ_n, energy gaps Δ_p and Δ_n, reciprocal moment of inertia $\hbar^2/2\mathcal{I}$, excitation energy of γ-vibration E_γ, the matrix element of γ between the vacuum and γ-vibration b, and the strength of p-n quadrupole interaction χ. Experimental values are first given to them, when available, and kept throughout fixed or varied slightly to obtain a good fit to the data. Energy gaps are derived from the binding energies of the neighboring nuclei[22] and are kept fixed. We use the average of deformations of the neighboring even nuclei obtained from $B(E2)$'s (Ref. 23) as a starting value of the deformation β and vary it to some extent to achieve a good fit to the experimental data. The values of β actually used are listed in Table I together with the starting values. The starting values of the Fermi energies are obtained by putting the selected

TABLE I. The values of the parameters used. We have started with the values listed in the lower column for β, λ's, and $\hbar^2/2\mathcal{I}$. They are obtained from the $B(E2)$ measured for the neighboring even-even nuclei (Ref. 23), by putting the proper neutron and proton numbers in the ordinary Nilsson diagram and from the energy spectra of the adjacent even-even nuclei. Then they are varied to obtain a good fit to the experimental data. The values actually used are given in the upper column. λ's are given in the form of $[n,\sigma]$ where $\lambda=\epsilon_n+\sigma(\epsilon_{n+1}-\epsilon_n)$ with n taking on 1,2,3, . . . , for $\Omega=\frac{1}{2},\frac{3}{2},\frac{5}{2},\ldots$. Δ's are estimated from the binding energies of the adjacent even-even and odd-A nuclei, and kept fixed. E_γ's are the average of the experimental excitation energies of γ-vibration in the adjacent even-even nuclei (Ref. 24). b^2 is about 1.6 times of the measured values for ^{154}Gd (Ref. 25).

	β	λ_p	λ_n	$\frac{\hbar^2}{2\mathcal{I}}$ (MeV)	Δ_p (MeV)	Δ_n (MeV)	E_γ (MeV)	b^2
$^{155}_{67}$Ho$_{88}$	0.23	[3,0.8]	[1,−1.0]	0.045	1.4	1.1	1.03	0.06
	(0.21)	([4,0.0])	([1,−0.5])	(0.057)				
$^{157}_{67}$Ho$_{90}$	0.27	[3,0.9]	[2,0.0]	0.024	1.2	1.3	0.89	0.06
	(0.27)	([4,0.0])	([2,0.0])	(0.028)				
$^{159}_{69}$Tm$_{90}$	0.25	[4,0.0]	[1,0.0]	0.031	1.3	1.2	0.82	0.06
	(0.24)	([4,0.3])	([2,0.0])	(0.036)				
$^{161}_{71}$Lu$_{90}$	0.22	[4,0.2]	[1,0.0]	0.035	1.3	1.2	0.82	0.06
	(0.21)	([4,0.4])	([1,0.0])	(0.044)				
$^{163}_{71}$Lu$_{92}$	0.25	[4,0.2]	[2,0.0]	0.029	1.2	1.2	0.84	0.06
	(0.24)	([4,0.5])	([2,0.0])	(0.031)				
$^{165}_{71}$Lu$_{94}$	0.27	[4,0.2]	[2,0.2]	0.024	1.2	1.2	0.86	0.06
	(0.27)	([4,0.6])	([2,0.5])	(0.024)				

deformation and proton or neutron number on the Nilsson diagram. Then we varied them in the neighborhood of the starting values to achieve a good agreement between the calculated and experimental spectra. The starting and the employed values are listed in Table I. Excitation energies of γ-vibration are taken from the observed values in the neighboring even nuclei.[24] We need $B(E2;2_\gamma^+ \rightarrow 0_g^+)$ of the neighboring even-even nuclei to fix b^2:

$$b = \left[\frac{B(E2;2_\gamma^+ \rightarrow 0_g^+)}{B(E2;2_g^+ \rightarrow 0_g^+)} \right]^{1/2} . \tag{3.1}$$

In some nuclei $B(E2;2_\gamma^+ \rightarrow 0_g^+)$'s have been measured: $b^2=0.038\pm0.001$ (^{154}Gd),[25] 0.025 ± 0.001 (^{156}Gd),[26] 0.017 ± 0.002 (^{158}Gd),[27] 0.014 ± 0.004 (^{160}Dy),[28] 0.026 ± 0.002 (^{166}Er).[29] We have found that these values are too small to reproduce the signature inversion in our model and used $b^2=0.06$. The use of a value for b^2 larger than measured may be justified to some extent as follows. We have introduced only one state to represent γ-vibration, while its strength is actually fragmented over several states. It is, therefore, reasonable to assign a larger value than measured to b^2 in order to let the γ-vibrational state introduced represent the actually fragmented strengths. We assume the following value for χ:

$$\chi = \frac{\pi V_1}{A\langle r^4 \rangle} + \frac{4\pi}{5} \frac{M\omega_0^2}{A\langle r^2 \rangle} , \tag{3.2}$$

where $V_1=130$ MeV, $\langle r^4 \rangle = 0.95 A^{4/3}$ fm^4, $\langle r^2 \rangle = 0.87 A^{2/3}$ fm^2, and $\hbar\omega_0 = 41 A^{-1/3}$ MeV. This was suggested by Bohr and Mottelson,[30] and gives $\chi \sim 0.004$ MeV/fm^4 for $A \sim 160$. Finally the moment of inertia at equilibrium $\hbar^2/2\mathcal{I}(\beta,\gamma=0°)$ is varied around the value obtained from the ground-state rotational bands of the neighboring even nuclei. The starting and employed values are listed in Table I. It is satisfying that the phenomenologically varied values are not far from the starting values. It should be noted that good parameter values are searched phenomenologically referring only to the energy spectra but not to other observables such as $B(M1)$'s.

B. Energy spectra

The calculated energy spectra are presented in Fig. 2. We readily see that the characteristic signature inversion after the band crossing is reproduced in agreement with experimental data for all the nuclei studied here. The correspondence between theory and experiment is best for ^{157}Ho and good for ^{163}Lu and ^{165}Lu. The theoretical result becomes less satisfactory compared with experiment for ^{159}Tm and ^{161}Lu and possibly for ^{155}Ho where the experimental information is insufficient. It is appropriate to say that the correspondence becomes poorer for nuclei where the energy spectra deviate more from the rigid rotor spectra. The general trend of Θ_I is rather flat in the experimental data while it increases with I in

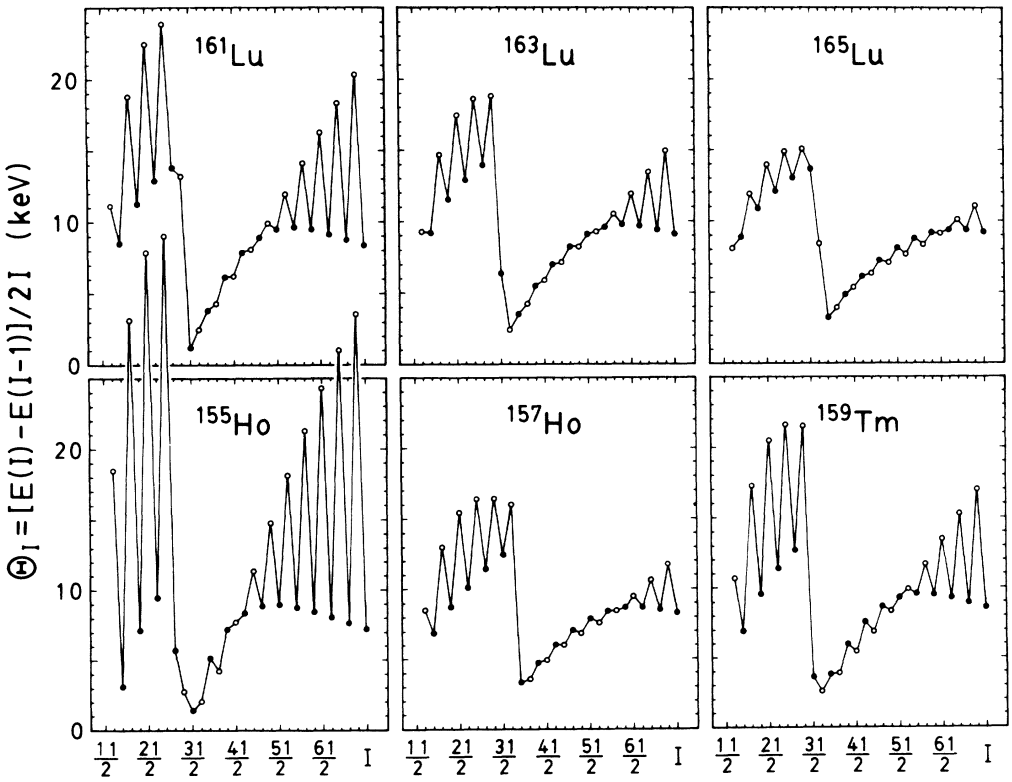

FIG. 2. Calculated energy spectra which are to be compared with Fig. 1. See Table I for values employed for the parameters.

the theory. This disagreement is supposed to come mainly from the assumption of rigid rotation in the model. Aside from this limitation, it is remarkable that the anomaly is described in terms of the present simple model. We denote the wave functions obtained here as $\Psi_{\text{L-a-S}}$, which we naturally propose as proper wave functions.

This overall success gives strong support to the present model and motivates us to look into it in more detail. We calculate the expectation values of the various terms of the Hamiltonian with the wave functions obtained and display the results for ^{157}Ho in Fig. 3 in the form of

$$\Theta_I(H_i) \equiv [\langle I|H_i|I\rangle - \langle I-1|H_i|I-1\rangle]/(2I) , \qquad (3.3)$$

where H_i is either H_{rot}, $H_{\text{q.p.}}$, H_γ, or H_{pn}. We immediately notice that H_{rot} works to produce the normal signature dependence in the present calculation as is expected, and that the oscillation of $\Theta_I(H_{\text{rot}})$ grows with spin. What we see here is the well-known effect of the Coriolis interaction. On the other hand, the quasiparticle energy term $\langle H_{\text{q.p.}}\rangle$ is found to work for the anomalous signature dependence. This can be understood as follows. First we should note that the rotor carries an extra amount of angular momentum in an unfavored state. This is because the difference of the total spin I and the particle spin j, $|I-j|$, is an odd integer in an unfavored state; while the spins of the ground-state band of the rotor, which constitutes dominant components in an odd-A nucleus over the γ band, are even integers so that the minimum value of the rotor spin, $R_{\min}$, is $I-j+1$ in an unfavored state and $I-j$ in a favored state. This means that the particle has more freedom in its orientation within the given geometry between I, R, and j in unfavored states. The particle or particles probably make use of this extra freedom to lower the quasiparticle energy in unfavored states more than in favored states. We find that $\langle H_{pn}\rangle$ works to produce the anomalous signature dependence also, although its magnitude is small. It is important to note that $\langle H_\gamma\rangle$ makes a large contribution to the signature inversion and that the oscillation of $\Theta_I(H_\gamma)$ grows with spin at almost the same pace as that of $\Theta_I(H_{\text{rot}})$. Thus the inverse signature dependence coming from $\langle H_\gamma\rangle$ competes with the normal signature dependence produced by $\langle H_{\text{rot}}\rangle$ over a wide range of spins. This behavior is essential for the successful reproduction of the signature inversion in the present model. We show $\Theta_I(H_{\text{q.p.}}+H_\gamma+H_{pn})$ by dotted lines in Fig. 3, which is seen to overcome $\Theta_I(H_{\text{rot}})$.

We are very much interested in how the γ-vibrational excitation and the γ dependence of the moments of inertia influence various physical observables. To study such effects, we prepare two other kinds of wave functions (1) by excluding the γ-vibrational excitation from the space or (2) by replacing the L-a-S moments of inertia with the IRF ones. In both cases the same values as given in Table I are assumed for the parameters. We denote the wave functions thus obtained as $\Psi_{\text{no-}\gamma}$ and Ψ_{IRF}. Obviously these wave functions do not describe the energy spectrum well but are expected to serve for comparative studies. To avoid confusion we remark again that it is

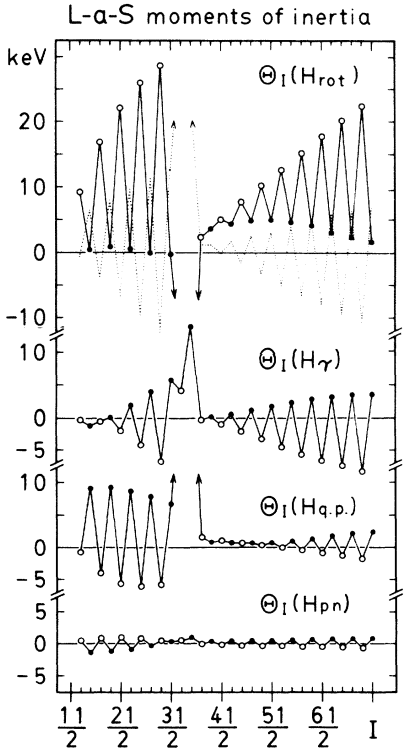

FIG. 3. Expectation values of H_{rot}, H_γ, $H_{\text{q.p.}}$, and H_{pn}, in the form of $\Theta_I(H_i)$ for ^{157}Ho. See the text for their definition [Eq. (3.3)]. This is a decomposition of the spectrum shown in Fig. 2 and naturally the L-a-S moments of inertia are used.

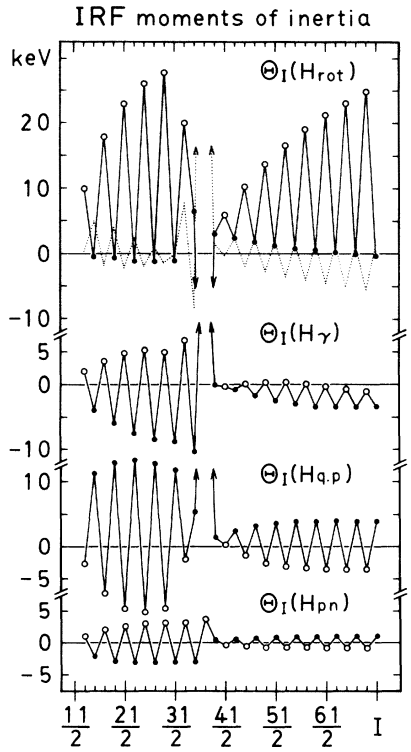

FIG. 4. The same quantities as given in Fig. 3 but the IRF moments of inertia are used. In contrast to Fig. 3, H_{rot} shows a stronger normal signature dependence and H_γ has a normal signature dependence.

$\Psi_{\text{L-a-S}}$ that we propose as proper wave functions.

We have calculated the quantities of Eq. (3.3) with the wave functions Ψ_{IRF} and illustrate them in Fig. 4. This is to be compared with Fig. 3. One can see that this time $\Theta_I(H_\gamma)$ makes a contribution to the normal signature dependence. This is a fundamental difference between the use of the IRF moments of inertia and that of the L-a-S ones, and this is why we need the L-a-S moments of inertia. It is desirable to understand in a non-numeric way how the signature dependence is related with the γ dependence of the moments of inertia employed. This remains to be studied.

C. Magnetic dipole transitions

A great deal of observed magnetic dipole ($M1$) transitions connecting favored and unfavored rotational levels show pronounced regular signature dependence. The observed signature dependence is such that $B(M1;I\to I-1)$'s from favored to unfavored are larger than those from unfavored to favored. The $M1$ transition operator consists of the angular momentum operators of the constituents and its matrix element between $\Omega=\frac{1}{2}$ and $\Omega=-\frac{1}{2}$ in the particle-rotor model contains the same phase factor as that of the Coriolis coupling. Thus the $M1$ transition is an observable that depends on signature as the energy spectrum does and it has been rather well understood with the simple particle-rotor model. Now we know that some nuclei show signature inversion in their energy levels and that it can be understood if the γ-vibrational excitation is taken into account and if the moments of inertia with a specific property are assumed. Then it is very interesting to see how the γ-vibrational excitation and specific dependence on γ of the moments of inertia influence $M1$ transitions. Thus we have calculated $M1$ transition probabilities using the wave functions obtained. We illustrate the result in Fig. 5 together with the available experimental data.

First of all we should note that the $B(M1)$'s calculated are in good agreement with experimental data with respect to order-of-magnitude values both below and above the band crossing in all the nuclei where experimental data are available.

We will compare the $B(M1)$'s calculated in more detail with experimental data. Below the band crossing, the $B(M1)$'s calculated have the normal signature dependence for all the nuclei in good agreement with experimental data. The signature dependence of the $B(M1)$'s calculated compares well with the experimental data for ^{161}Lu and ^{165}Lu. The dependence looks somewhat too large for ^{157}Ho and too small for ^{159}Tm compared with the data.

The signature dependence of the $B(M1)$'s calculated is seen not to be normal in some nuclei for a few transitions immediately after the band crossing, as in the $\frac{35}{2}\to\frac{33}{2}$, $\frac{33}{2}\to\frac{31}{2}$, and $\frac{31}{2}\to\frac{29}{2}$ transitions of ^{155}Ho. Except for these few transitions, the $B(M1)$'s calculated show the normal signature dependence after the band crossing as well as before it.

The experimental data on ^{157}Ho obtained by Radford *et al.*[10] show the normal signature dependence in 12 transitions out of the 14 transitions from $\frac{63}{2}\to\frac{61}{2}$ to $\frac{37}{2}\to\frac{35}{2}$ except for the two transitions of $\frac{55}{2}\to\frac{53}{2}$ and $\frac{43}{2}\to\frac{41}{2}$. This agreement gives strong support to the present model.

On the other hand the theoretical results do not seem

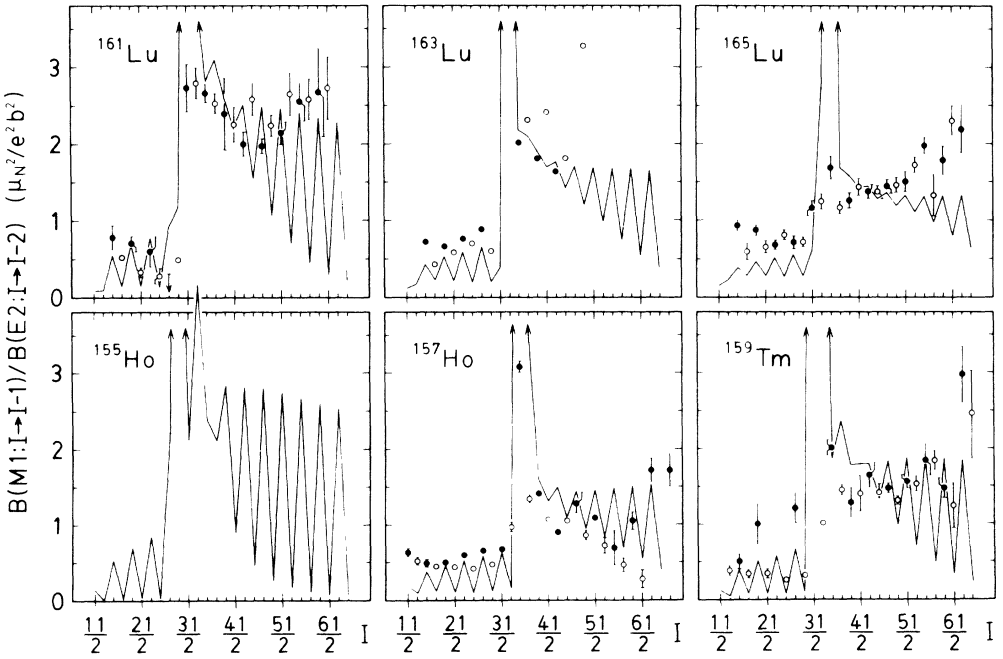

FIG. 5. Calculated and experimental $B(M1;I\to I-1)/B(E2;I\to I-2)$ along the negative parity yrast bands of ^{155,157}Ho, ^{159}Tm, and ^{161,163,165}Lu. Experimental data are taken from Ref. 10 for ^{157}Ho, Ref. 5 for ^{159}Tm, Ref. 12 for ^{161}Lu, Ref. 13 for ^{163}Lu, and Ref. 17 for ^{165}Lu.

in accord with the experimental data on ^{161}Lu that show inverted signature dependence for the 7 transitions from $\frac{53}{2} \rightarrow \frac{51}{2}$ to $\frac{41}{2} \rightarrow \frac{39}{2}$. This is the only case where the present calculation disagrees with experimental data. In the present model we assign specific numerical values to the parameters by referring to the energy spectra. Since the level schemes of the nuclei under study are quite similar to each other, the adopted values of the parameters are similar and we obtain from them wave functions which vary gradually from nucleus to nucleus. Therefore, it is improbable that completely opposite signature dependences will be predicted for ^{157}Ho and ^{161}Lu in the present theoretical framework.

Now we investigate how the γ-vibrational excitation and the dependence on γ of moments of inertia affect the dependence of $M1$ transitions on signature. For this purpose we have calculated the $M1$ transition strengths using the wave functions Ψ_{IRF} and $\Psi_{\text{no-}\gamma}$ for the case of ^{157}Ho, and illustrate the results in Fig. 6 for comparison together with those already given in Fig. 5 which were calculated with $\Psi_{\text{L-a-S}}$. Immediately we notice in the figure that the γ dependence of the moments of inertia has a close relation with the dependence of the $M1$ transitions on signature: if the γ-vibrational excitation is not taken into account, the $M1$ transitions show a pronounced normal signature dependence. If the IRF moments of inertia are used, the γ-vibrational excitation works to enhance the normal signature dependence of the $M1$ transitions. On the other hand, if the L-a-S moments of inertia are used, the γ-vibrational excitation seems to reduce, or even to invert at least instantaneously, the normal signature dependence in the $M1$ transitions. This effect to reduce or to invert the normal signature dependence of the $M1$ transitions is, however, not very large so that the signature dependence of the $M1$ matrix elements gets reduced in magnitude but remains normal except for a small region of spin after the band crossing in a few cases.

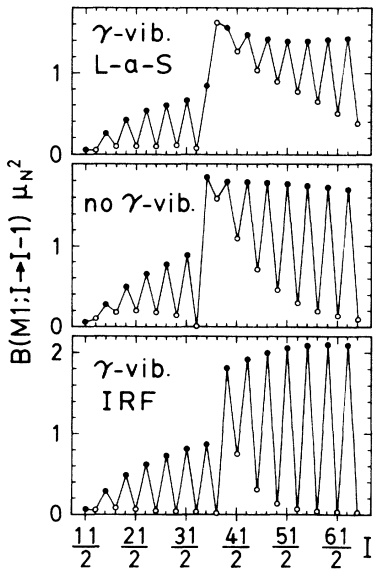

FIG. 6. Comparison of the effects of γ-vibration and different sets of moments of inertia on $B(M1)$'s. $B(M1)$'s calculated with or without the γ-vibrational excitation, and with different sets of moments of inertia. The γ-vibrational excitation influences signature dependence of $B(M1)$'s differently with different moments of inertia.

D. Electric quadrupole transitions

Electric quadrupole ($E2$) transition probabilities with a spin change of $1\hbar$ were measured for ^{157}Ho some years ago and it was reported that quite strong signature dependence was observed in $B(E2;I \rightarrow I-1)$'s; $B(E2;I,$ favored$\rightarrow I-1,$unfavored) are much stronger than $B(E2;I,$unfavored$\rightarrow I-1,$favored) before the band crossing as well as after it. This report motivated theoretical studies on the signature dependence of the $B(E2;I \rightarrow I-1)$'s. Calculations were carried out in the model of a quasiparticle coupled to a triaxial rotor and it was concluded that such signature dependence is evidence that the nucleus has an equilibrium triaxial shape.[19] Then the problem was studied in the model of a quasiparticle coupled to an axially symmetric rotor which undergoes γ-vibration.[20] It was found that the dynamical fluctuation in the γ direction gives rise to rather strong signature dependence in the $B(E2)$'s, which is of the same size as that obtained by assuming a permanent triaxial deformation. However, both of the models predicted a weaker signature dependence of the $B(E2)$'s than was measured. Recently Radford *et al.* performed a spectroscopic experiment on ^{157}Ho and measured various observables including the $B(E2;I \rightarrow I-1)$'s.[10] The newly obtained $B(E2;I \rightarrow I-1)$'s show a weaker dependence on the signature than those of the previous experiment, with no obvious discrepancy with the predictions of the dynamical or the static triaxial models.

Now in this study we ascertain that the IRF moments of inertia are not appropriate in γ dependence, and that a correct set of moments of inertia must be the L-a-S ones. In Ref. 20, however, the IRF moments of inertia were adopted and rather strong signature dependence was pre-

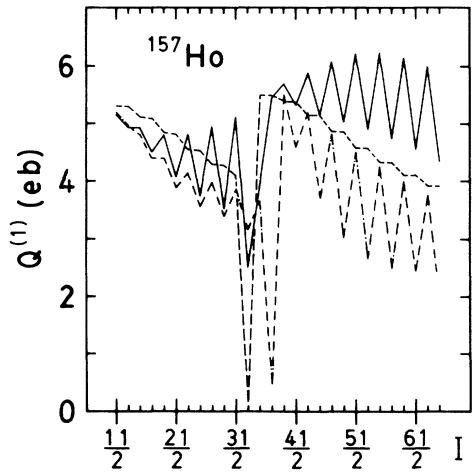

FIG. 7. $B(E2;I \rightarrow I-1)$'s for ^{157}Ho in the form of $Q^{(1)}$ calculated with different models: with the γ-vibrational degree of freedom with the L-a-S (full line) or IRF (dash-dotted line) moments of inertia and without it (dashed line).

dicted for the $B(E2;I\rightarrow I-1)$'s. Thus we might ask whether the conclusion of Ref. 20 is still correct or not and whether different signature dependences are predicted or not for the $B(E2;I\rightarrow I-1)$'s with the L-a-S moments. We have calculated the $B(E2;I\rightarrow I-1)$'s with the wave functions $\Psi_{\text{L-a-S}}$ as well as Ψ_{IRF} and $\Psi_{\text{no-}\gamma}$, and the results are presented in Fig. 7 in the form of $Q^{(1)}$ which is defined as

$$Q^{(i)}=\left[\frac{16\pi}{5}\frac{B(E2;I\rightarrow I-i)}{(IK20|I-iK)^2}\right]^{1/2} \quad (i=1,2)\ , \qquad (3.4)$$

where K is set equal to $\frac{7}{2}$ for ^{157}Ho. As was found in Refs. 19 and 20, the particle plus symmetric rotor model without the γ-vibrational excitation predicts practically no signature dependence in the $B(E2;I\rightarrow I-1)$'s. We find that $\Psi_{\text{L-a-S}}$ as well as Ψ_{IRF} predict quite similar and recognizable signature dependence in the $B(E2)$'s, i.e., the $B(E2;I\rightarrow I-1)$'s are predicted to be larger for the f (favored) to u (unfavored) transitions than for u to f by both of them. There are two different features between the $B(E2;I\rightarrow I-1)$'s calculated with $\Psi_{\text{L-a-S}}$ and Ψ_{IRF}. One is that the signature dependence predicted by $\Psi_{\text{L-a-S}}$ is larger than that by Ψ_{IRF} before the band crossing, i.e.,

$$\frac{Q^{(1)}_{f\rightarrow u}-Q^{(1)}_{u\rightarrow f}}{(Q^{(1)}_{f\rightarrow u}+Q^{(1)}_{u\rightarrow f})/2}\ , \qquad (3.5)$$

reaches approximately 37% in the case of $\Psi_{\text{L-a-S}}$ while only 20% for Ψ_{IRF}. The other is that the $B(E2)$'s decrease more rapidly for Ψ_{IRF} than for $\Psi_{\text{L-a-S}}$.

In Fig. 8 we present the results calculated with $\Psi_{\text{L-a-S}}$ for all the isotopes studied in this paper together with the experimental data for ^{159}Tm.[6] We notice that the $B(E2;I\rightarrow I-1)$'s predicted look quite similar for all the isotopes. We observe also a sort of regularity in the $B(E2)$'s. This is a reflection of the similarity and regularity of their energy spectra. Unfortunately the experimental information is not sufficient enough to say anything conclusive about the regularity. In Fig. 9 we illustrate $Q^{(1)}/Q^{(2)}$ for ^{157}Ho and ^{165}Lu for which experimental data are available.[10,17] Although the theoretical values are within the error bars, it is hard to derive a meaningful conclusion from the comparison because of large error bars.

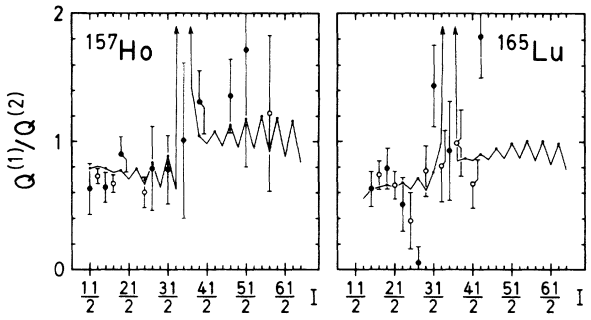

FIG. 9. Calculated and experimental $B(E2;I\rightarrow I-1)/B(E2;I\rightarrow I-2)$ for ^{157}Ho and ^{165}Lu in the form of $Q^{(1)}/Q^{(2)}$, where K is set equal to $\frac{7}{2}$ for ^{157}Ho and $\frac{9}{2}$ for ^{165}Lu. Experimental data are taken from Ref. 10 for ^{157}Ho and Ref. 17 for ^{165}Lu.

We will see how $B(E2;I\rightarrow I-2)$'s are influenced by the γ-vibrational excitation. In Fig. 10 we show the $B(E2;I\rightarrow I-2)$'s calculated with $\Psi_{\text{L-a-S}}$, Ψ_{IRF}, and $\Psi_{\text{no-}\gamma}$ in the form of $Q^{(2)}$. The γ-vibrational excitation gives rise to weak but noticeable signature dependence in $Q^{(2)}$ before the band crossing. The difference, $Q^{(2)}_{f\rightarrow f}-Q^{(2)}_{u\rightarrow u}$, does not exceed 8% of their average. In Fig. 11 we present our prediction for the $Q^{(2)}$'s together with experi-

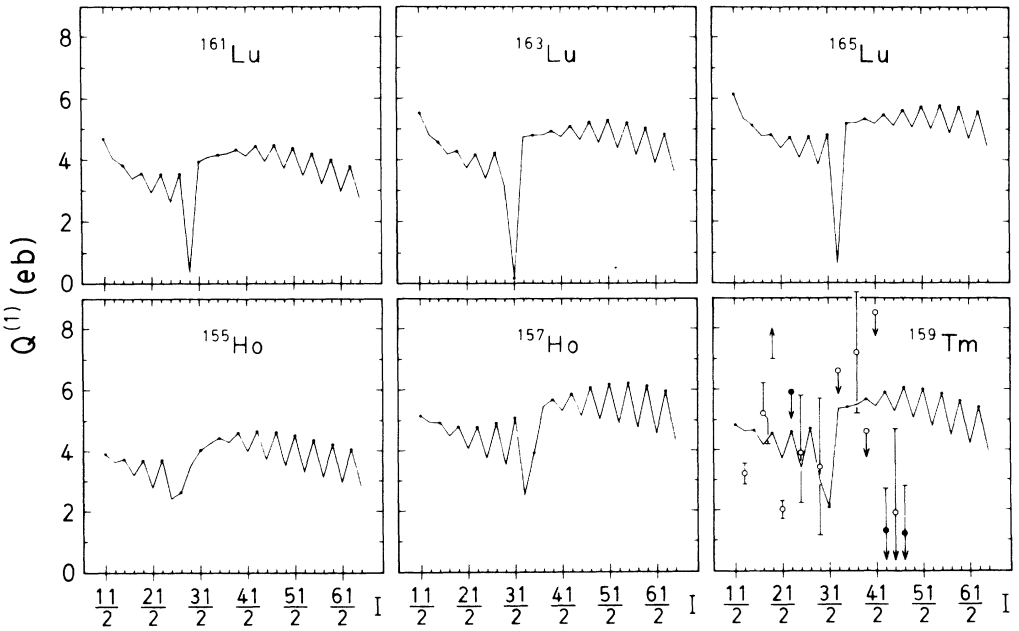

FIG. 8. Calculated $B(E2;I\rightarrow I-1)$'s in the form of $Q^{(1)}$ and experimental data (Ref. 6). K appearing in $Q^{(1)}$ [see Eq. (3.4)] is set equal to $\frac{7}{2}$ for ^{155,157}Ho and ^{159}Tm and $\frac{9}{2}$ for ^{161,163,165}Lu.

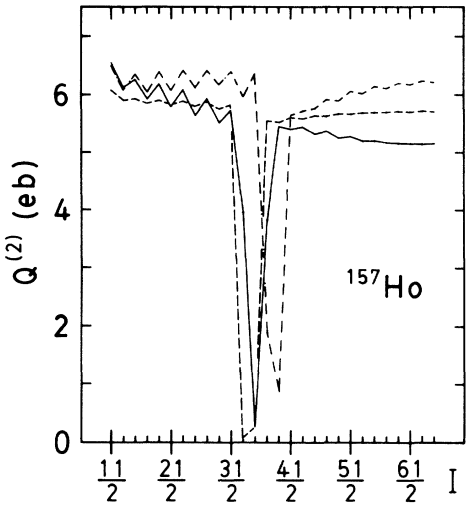

FIG. 10. $B(E2;I\rightarrow I-2)$'s in the form of $Q^{(2)}$ calculated with or without the γ-vibrational excitation and with different sets of moments of inertia. The dashed line represents the calculations without γ-vibrational excitation. Both of full and dash-dotted lines show the calculations with the γ-vibrational excitation with the L-a-S or the IRF moments of inertia, respectively.

mental data for ^{157}Ho[11] and ^{159}Tm.[6] The prediction and the experimental data are consistent in the sense that they do not show any strong signature dependence, but are not in the sense that the experimental data on ^{157}Ho seem to indicate quite irregular behavior around $I=\frac{17}{2}$, $I=\frac{43}{2}$, and $I=\frac{51}{2}$ while the theoretical values vary regularly with spin.

IV. SUMMARY AND CONCLUSION

We have performed a numerical study in the framework of the model proposed in a previous paper with the intention of determining whether the model contains in it the essential degrees of freedom involved in the signature inversion observed in the light Ho, Tm, and Lu isotopes by applying it to various nuclei.

The model is an extended version of the particle-rotor model. The system is assumed to have an axially symmetric equilibrium deformation and to undergo γ-vibration around it. Two types of configurations are explicitly taken into account: an $h_{11/2}$ quasiproton is present in one and two $i_{13/2}$ quasineutrons in addition to an $h_{11/2}$ quasiproton in the other. These configurations are necessary to describe the proton $h_{11/2}$ band of the nuclei of interest and its band crossing. We have first calculated the energy spectra of ^{155,157}Ho, ^{159}Tm, and ^{161,163,165}Lu by employing the Largest-around-Shortest moments of inertia, and successfully reproduced the signature inversion of these isotopes by adjusting the involved parameters to some extent. It should be noted that the adopted values of the parameters are all around what are expected from circumstances. These successful results give strong support to the conclusion derived in the previous paper: the γ dependence of the moments of inertia influence the signature dependence of the energy spectra decisively and the irrotational flow model moments of inertia are inappropriate. The appropriate γ dependence of the moments of inertia is such that the largest one is around the shortest axis of a triaxially deformed shape and the next to the largest is around the

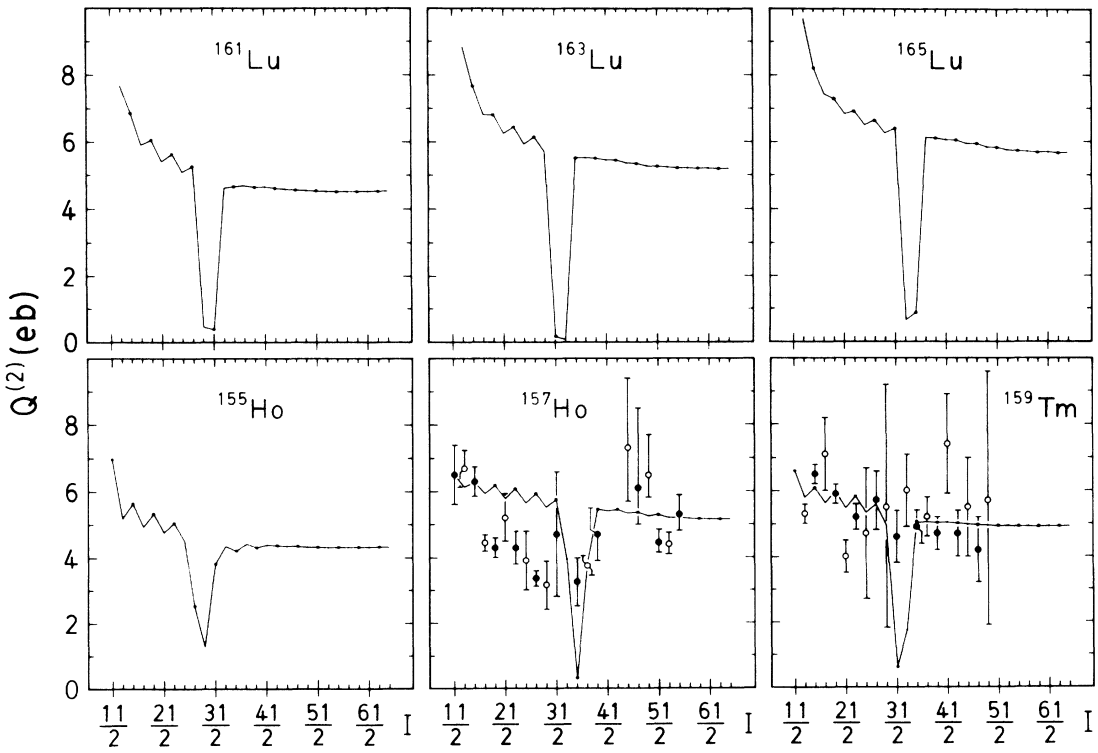

FIG. 11. Calculated and experimental $Q^{(2)}$. $K=\frac{7}{2}$ is given to ^{155,157}Ho, ^{159}Tm, and $K=\frac{9}{2}$ to ^{161,163,165}Lu. Experimental data are taken from Ref. 11 for ^{157}Ho and Ref. 6 for ^{159}Tm.

axis of intermediate length. Up to recently we had practically no knowledge about the γ dependence of the moments of inertia. We have learned through the present study that the signature inversion observed in these nuclei provides an opportunity to discuss this subject.

We have obtained the wave functions by referring only to the energy spectra concerned. It is, therefore, interesting and meaningful to see what the model predicts for other observables and to see how the predictions compare with experimental data when available. First we have studied $B(M1;I\rightarrow I-1)$. When we calculate $B(M1)$'s with no γ-vibrational excitation taken into account, they are predicted to have quite a strong normal signature dependence. If we take into account the γ-vibrational excitation and assume the IRF moments of inertia we see an enhancement of the normal signature dependence in the calculated $B(M1)$'s. If the γ-vibrational excitation is considered in combination with the L-a-S moments of inertia we find that the calculated $B(M1)$'s have normal but weaker signature dependence. Thus the γ-vibrational degree of freedom works to enhance or reduce the normal signature dependence depending on the moments of inertia employed. A very important point of the results is that the predicted signature dependence of the $B(M1)$'s is normal everywhere before and after the band crossing in most nuclei studied. There are a few exceptions where a few transitions just above the band crossing show the inverted signature dependence. Thus, the present model almost always predicts the normal signature dependence for the $B(M1)$'s in spite of the signature inversion in the energy spectra. This prediction is in good agreement with the experimental data on ^{157}Ho. The agreement is good for ^{159}Tm also. The result for ^{161}Lu seems to disagree with the data. It is inevitable that the present theory predicts very similar behaviors of $B(M1)$'s for ^{157}Ho and for ^{161}Lu, because the wave functions are generated by referring only to their energy spectra which are quite similar to each other. The present theory predicts an appreciable amount of increase of the $B(M1)$'s at the band crossing in association with the rotation alignment of $(vi_{13/2})^2$ quasiparticles. This is in excellent agreement with all the experimental data.

We have then calculated $B(E2;I\rightarrow I-1)$ with the wave functions obtained. An important feature of the calculated $B(E2)$'s is that the γ-vibrational excitation gives rise to an appreciable amount of signature dependence and that quite similar signature dependences are obtained with either the IRF moments of inertia or the L-a-S moments of inertia. No disagreement is observed between the calculated $B(E2)$'s and the experimental data. The $B(E2)$'s must be measured with higher precision for more critical discussion.

In conclusion, the present study has shown that the characteristic signature inversion of the energy spectra of the Ho, Tm, Lu isotopes as well as most of the $M1$ and $E2$ transition probabilities can be described by taking into account the γ-vibrational excitation around an axially symmetric deformation and assuming the L-a-S moments of inertia.

ACKNOWLEDGMENTS

We thank Sam Tabor of Florida State University for reading the manuscript carefully and giving us valuable comments. The numerical calculations were carried out with the S-820, M-680H, and M-682H computer systems at the Computer Centre, University of Tokyo. This work has been partially supported by the Grant-in-Aid for Scientific Research of the Japan Ministry of Education, Science, and Culture under Grants Nos. 62540198 and 62302014.

APPENDIX A: MATRIX ELEMENTS OF HAMILTONIAN

In this appendix we give explicit forms of the matrix elements of the Hamiltonian. To express these matrix elements compactly we define the following abbreviations:

$$E_{j_\tau\mu}\equiv\sqrt{(\epsilon_{j_\tau\mu}-\lambda_\tau)^2+\Delta_\tau^2}\quad(\tau=p,n)\,, \tag{A1}$$

$$(uu)^\tau_\mu\equiv(u_{j_\tau\mu}u_{j_\tau\mu-1}+v_{j_\tau\mu}v_{j_\tau\mu-1})\sqrt{j_\tau(j_\tau+1)-\mu(\mu-1)}\quad(\tau=p,n)\,, \tag{A2}$$

$$(uv)^\tau_\mu\equiv(-1)^{j_\tau-\mu}(u_{j_\tau\mu}v_{j_\tau\mu-1}-v_{j_\tau\mu}u_{j_\tau\mu-1})\sqrt{j_\tau(j_\tau+1)-\mu(\mu-1)}\quad(\tau=p,n)\,, \tag{A3}$$

$$[(uu)^2]^\tau_\mu\equiv\tfrac{1}{2}\{[(uu)^\tau_\mu]^2+[(uu)^\tau_{\mu+1}]^2-[(uv)^\tau_\mu]^2-[(uv)^\tau_{\mu+1}]^2\}\quad(\tau=p,n)\,, \tag{A4}$$

$$[(uu)(uu)]^\tau_\mu\equiv\tfrac{1}{2}[(uu)^\tau_\mu(uu)^\tau_{\mu-1}-(uv)^\tau_\mu(uv)^\tau_{\mu-1}]\quad(\tau=p,n)\,, \tag{A5}$$

$$[(uu)(uv)]^n_\mu\equiv\tfrac{1}{2}[(uu)^n_\mu(uv)^n_{\mu-1}+(uv)^n_\mu(uu)^n_{\mu-1}]\,, \tag{A6}$$

$$\langle uu\rangle^\tau_\mu\equiv(u_{j_\tau\mu}u_{j_\tau\mu-2}-v_{j_\tau\mu}v_{j_\tau\mu-2})\langle j_\tau,\mu-2|Y_{2,-2}|j_\tau\mu\rangle\quad(\tau=p,n)\,, \tag{A7}$$

$$\langle uv\rangle^n_\mu\equiv(-1)^{j_n+\mu}(u_{j_n\mu}v_{j_n\mu-2}+v_{j_n\mu}u_{j_n\mu-2})\langle j_n,\mu-2|Y_{2,-2}|j_n\mu\rangle\,, \tag{A8}$$

$$V_{pn}(\rho';\rho\sigma\tau)\equiv(-1)^{j_n-\tau}(u_{j_p\rho'}u_{j_p\rho}u_{j_n\sigma}v_{j_n\tau}-v_{j_p\rho'}v_{j_p\rho}v_{j_n\sigma}u_{j_n\tau})\langle j_p\rho',j_n\tau|V_{pn}|j_p\rho,j_n\sigma\rangle\,, \tag{A9}$$

$$\begin{aligned}V_{pn}(\rho'\sigma';\rho\sigma)\equiv&(u_{j_p\rho'}u_{j_n\sigma'}u_{j_p\rho}u_{j_n\sigma}+v_{j_p\rho'}v_{j_n\sigma'}v_{j_p\rho}v_{j_n\sigma})\langle j_p\rho',j_n\sigma'|V_{pn}|j_p\rho,j_n\sigma\rangle\\&-(-1)^{\sigma'-\sigma}(u_{j_p\rho'}v_{j_n\sigma'}u_{j_p\rho}v_{j_n\sigma}+v_{j_p\rho'}u_{j_n\sigma'}v_{j_p\rho}u_{j_n\sigma})\langle j_p\rho',j_n-\sigma|V_{pn}|j_p\rho,j_n-\sigma'\rangle\,.\end{aligned} \tag{A10}$$

In the formula below the quantum numbers, Λ and n, are to specify the wave functions of γ variable.

(i) Matrix elements between one-quasiproton states ($K'=\rho'+\Lambda'>0$, $K=\rho+\Lambda>0$, $K'\le K$):

$$\begin{aligned}
\langle \Psi^{IMK'}_{\rho',\Lambda'n'}|H|\Psi^{IMK}_{\rho,\Lambda n}\rangle &= \delta_{K'K}\delta_{\rho'\rho}\delta_{\Lambda'\Lambda}\delta_{n'n}\left[E_{j_p\rho}+E^{\gamma}_{\Lambda n}+\frac{\hbar^2}{2\mathcal{J}}[I(I+1)-K^2]+\frac{\hbar^2}{2\mathcal{J}}[(uu)^2]^p_{\rho}\right] \\
&-\frac{\hbar^2}{2\mathcal{J}}[\delta_{K',K-1}\delta_{\rho',\rho-1}\delta_{\Lambda'\Lambda}+(-1)^{I-j_p}\delta_{K'K}\delta_{K,1/2}\delta_{\rho',-\rho+1}\delta_{\Lambda',-\Lambda}]\delta_{n'n}\sqrt{I(I+1)-K(K-1)}(uu)^p_{\rho} \\
&-\frac{a_\gamma}{\sqrt{3}}\frac{\hbar^2}{2\mathcal{J}}[\delta_{K',K-2}\delta_{\rho'\rho}\delta_{\Lambda',\Lambda-2}+(-1)^{I-j_p}\delta_{K',-K+2}\delta_{\rho',-\rho}\delta_{\Lambda',-\Lambda+2}] \\
&\times\langle\Lambda-2,n'|\gamma|\Lambda n\rangle\sqrt{[I(I+1)-K(K-1)][I(I+1)-(K-1)(K-2)]} \\
&+\frac{2a_\gamma}{\sqrt{3}}\frac{\hbar^2}{2\mathcal{J}}[\delta_{K',K-1}\delta_{\rho',\rho+1}\delta_{\Lambda',\Lambda-2}+(-1)^{I-j_p}\delta_{K'K}\delta_{K,1/2}\delta_{\rho',-\rho-1}\delta_{\Lambda',-\Lambda+2}] \\
&\times\langle\Lambda-2,n'|\gamma|\Lambda n\rangle\sqrt{I(I+1)-K(K-1)}(uu)^p_{\rho+1} \\
&-\frac{2a_\gamma}{\sqrt{3}}\frac{\hbar^2}{2\mathcal{J}}\delta_{K'K}\{\delta_{\rho',\rho+2}\delta_{\Lambda',\Lambda-2}\langle\Lambda-2,n'|\gamma|\Lambda n\rangle[(uu)(uu)]^p_{\rho+2} \\
&\qquad+\delta_{\rho',\rho-2}\delta_{\Lambda',\Lambda+2}\langle\Lambda+2,n'|\gamma|\Lambda n\rangle[(uu)(uu)]^p_{\rho}\} \\
&+\frac{1}{\sqrt{2}}q_p\beta\delta_{K'K}(\delta_{\rho',\rho-2}\delta_{\Lambda',\Lambda-2}\langle\Lambda-2,n'|\gamma|\Lambda n\rangle\langle uu\rangle^p_{\rho+2} \\
&\qquad+\delta_{\rho',\rho-2}\delta_{\Lambda',\Lambda+2}\langle\Lambda+2,n'|\gamma|\Lambda n\rangle\langle uu\rangle^p_{\rho}) ,
\end{aligned} \tag{A11}$$

where $\Lambda=n=0$ stands for the ground state of γ-vibration and $\Lambda=\pm2$, $n=0$ for the state of one γ-vibrational quantum.

(ii) Matrix elements between one-quasiproton states and three-quasiparticles (one-quasiproton and two-quasineutron) states ($K'=\rho'+\Lambda'>0$, $K=\rho+\sigma+\tau+\Lambda>0$, $\sigma>\tau$):

$$\begin{aligned}
\langle \Psi^{IMK'}_{\rho',\Lambda'n'}|H|\Psi^{IMK}_{\rho,\sigma\tau,\Lambda n}\rangle &= \frac{\hbar^2}{2\mathcal{J}}\{[\delta_{K',K-1}\delta_{\rho'\rho}\delta_{\Lambda'\Lambda}+(-1)^{I-j_p}\delta_{K'K}\delta_{K,1/2}\delta_{\rho',-\rho}\delta_{\Lambda',-\Lambda}]\delta_{\sigma+\tau,1}\delta_{n'n} \\
&\qquad\times\sqrt{I(I+1)-K(K-1)}(uv)^n_{\sigma} \\
&\qquad+\delta_{K',K+1}\delta_{\rho'\rho}\delta_{\sigma+\tau,-1}\delta_{\Lambda'\Lambda}\delta_{n'n}\sqrt{I(I+1)-K(K+1)}(uv)^n_{\sigma+1}\} \\
&-\frac{\hbar^2}{2\mathcal{J}}\delta_{K'K}\delta_{\Lambda'\Lambda}\delta_{n'n}\{\delta_{\rho'\rho}\delta_{\sigma+\tau,0}[(uu)^n_{\sigma}(uv)^n_{\sigma}+(uu)^n_{\sigma+1}(uv)^n_{\sigma+1}] \\
&\qquad+\delta_{\rho',\rho+1}\delta_{\sigma+\tau,1}(uu)^p_{\rho+1}(uv)^n_{\sigma}+\delta_{\rho',\rho-1}\delta_{\sigma+\tau,-1}(uu)^p_{\rho}(uv)^n_{\sigma+1}\} \\
&-\frac{2a_\gamma}{\sqrt{3}}\frac{\hbar^2}{2\mathcal{J}}\{[\delta_{K',K-1}\delta_{\rho'\rho}\delta_{\Lambda',\Lambda-2}+(-1)^{I-j_p}\delta_{K'K}\delta_{K,1/2}\delta_{\rho',-\rho}\delta_{\Lambda',-\Lambda+2}]\delta_{\sigma+\tau,-1} \\
&\qquad\times\langle\Lambda-2,n'|\gamma|\Lambda n\rangle\sqrt{I(I+1)-K(K-1)}(uv)^n_{\sigma+1} \\
&\qquad+\delta_{K',K+1}\delta_{\rho'\rho}\delta_{\sigma+\tau,1}\delta_{\Lambda',\Lambda+2}\langle\Lambda+2,n'|\gamma|\Lambda n\rangle\sqrt{I(I+1)-K(K+1)}(uv)^n_{\sigma}\} \\
&+\frac{2a_\gamma}{\sqrt{3}}\frac{\hbar^2}{2\mathcal{J}}\delta_{K'K}\{\delta_{\rho'\rho}[\delta_{\sigma+\tau,-2}\delta_{\Lambda',\Lambda-2}\langle\Lambda-2,n'|\gamma|\Lambda n\rangle[(uu)(uv)]^n_{\sigma+2} \\
&\qquad+\delta_{\sigma+\tau,2}\delta_{\Lambda',\Lambda+2}\langle\Lambda+2,n'|\gamma|\Lambda n\rangle[(uu)(uv)]^n_{\sigma}] \\
&\qquad+\delta_{\rho',\rho+1}\delta_{\sigma+\tau,-1}\delta_{\Lambda',\Lambda-2}\langle\Lambda-2,n'|\gamma|\Lambda n\rangle(uu)^p_{\rho+1}(uv)^n_{\sigma+1} \\
&\qquad+\delta_{\rho',\rho-1}\delta_{\sigma+\tau,1}\delta_{\Lambda',\Lambda+2}\langle\Lambda+2,n'|\gamma|\Lambda n\rangle(uu)^p_{\rho}(uv)^n_{\sigma}\} \\
&-\frac{1}{\sqrt{2}}q_n\beta\delta_{K'K}\delta_{\rho'\rho}(\delta_{\sigma+\tau,-2}\delta_{\Lambda',\Lambda-2}\langle\Lambda-2,n'|\gamma|\Lambda n\rangle\langle uv\rangle^n_{\sigma+2} \\
&\qquad+\delta_{\sigma+\tau,2}\delta_{\Lambda',\Lambda+2}\langle\Lambda+2,n'|\gamma|\Lambda n\rangle\langle uv\rangle^n_{\sigma}) \\
&+\delta_{K'K}\delta_{\Lambda'\Lambda}\delta_{n'n}[V_{pn}(\rho';\rho\sigma-\tau)-V_{pn}(\rho';\rho\tau-\sigma)] .
\end{aligned} \tag{A12}$$

(iii) Matrix elements between three-quasiparticles (one-quasiproton and two-quasineutron) states ($K'=\rho'+\sigma'+\tau'+\Lambda'>0$, $\sigma'>\tau'$, $K=\rho+\sigma+\tau+\Lambda>0$, $\sigma>\tau$, $K'\le K$):

$$
\begin{aligned}
&\langle \Psi^{IMK'}_{\rho',\sigma'\tau',\Lambda'n'}|H|\Psi^{IMK}_{\rho,\sigma\tau,\Lambda n}\rangle \\
&=\delta_{K'K}\delta_{\rho'\rho}\delta_{\sigma'\sigma}\delta_{\tau'\tau}\delta_{\Lambda'\Lambda}\delta_{n'n}\left[E_{j_p\rho}+E_{j_n\sigma}+E_{j_n\tau}+E^{\gamma}_{\Lambda n}+\frac{\hbar^2}{2\mathcal{J}}[I(I+1)-K^2]\right] \\
&-\frac{\hbar^2}{2\mathcal{J}}\sqrt{I(I+1)-K(K-1)} \\
&\times\{\delta_{K',K-1}\delta_{\Lambda'\Lambda}\delta_{n'n}[\delta_{\rho',\rho-1}\delta_{\sigma'\sigma}\delta_{\tau'\tau}(uu)^p_\rho+\delta_{\rho'\rho}\delta_{\sigma',\sigma-1}\delta_{\tau'\tau}(uu)^n_\sigma+\delta_{\rho'\rho}\delta_{\sigma'\sigma}\delta_{\tau',\tau-1}(uu)^n_\tau] \\
&\quad+(-1)^{I-j_p}\delta_{K'K}\delta_{K,1/2}\delta_{\Lambda',-\Lambda}\delta_{n'n}[\delta_{\rho',-\rho+1}\delta_{\sigma',-\tau}\delta_{\tau',-\sigma}(uu)^p_\rho+\delta_{\rho',-\rho}\delta_{\sigma',-\tau}\delta_{\tau',-\sigma+1}(uu)^n_\sigma \\
&\qquad+\delta_{\rho',-\rho}\delta_{\sigma',-\tau+1}\delta_{\tau',-\sigma}(uu)^n_\tau]\} \\
&+\frac{\hbar^2}{2\mathcal{J}}\delta_{K'K}\delta_{\Lambda'\Lambda}\delta_{n'n}[\delta_{\rho'\rho}(\delta_{\sigma'\sigma}\delta_{\tau'\tau}\{[(uu)^2]^p_\rho+[(uu)^2]^2_\sigma+[(uu)^2]^n_\tau\} \\
&\qquad+(\delta_{\sigma',\sigma-1}\delta_{\tau',\tau+1}-\delta_{\sigma',\tau+1}\delta_{\tau',\sigma-1})(uu)^n_\sigma(uu)^n_{\tau+1}+\delta_{\sigma',\sigma+1}\delta_{\tau',\tau-1}(uu)^n_{\sigma+1}(uu)^n_\tau \\
&\qquad+\delta_{\sigma'+\tau',1}\delta_{\sigma+\tau,1}(uv)^n_{\sigma'}(uv)^n_\sigma+\delta_{\sigma'+\tau',-1}\delta_{\sigma+\tau,-1}(uv)^n_{\sigma'+1}(uv)^n_{\sigma+1}) \\
&\quad+\delta_{\rho',\rho+1}(uu)^p_{\rho+1}[\delta_{\sigma',\sigma-1}\delta_{\tau'\tau}(uu)^n_\sigma+\delta_{\sigma'\sigma}\delta_{\tau',\tau-1}(uu)^n_\tau] \\
&\quad+\delta_{\rho',\rho-1}(uu)^p_\rho[\delta_{\sigma',\sigma+1}\delta_{\tau'\tau}(uu)^n_{\sigma+1}+\delta_{\sigma'\sigma}\delta_{\tau',\tau+1}(uu)^n_{\tau+1}]] \\
&-\frac{a_\gamma}{\sqrt{3}}\frac{\hbar^2}{2\mathcal{J}}[\delta_{K',K-2}\delta_{\rho'\rho}\delta_{\sigma'\sigma}\delta_{\tau'\tau}\delta_{\Lambda',\Lambda-2}+(-1)^{I-j_p}\delta_{K',-K+2}\delta_{\rho',-\rho}\delta_{\sigma',-\tau}\delta_{\tau',-\sigma}\delta_{\Lambda',-\Lambda+2}] \\
&\times\langle\Lambda-2,n'|\gamma|\Lambda n\rangle\sqrt{[I(I+1)-K(K-1)][I(I+1)-(K-1)(K-2)]} \\
&+\frac{2a_\gamma}{\sqrt{3}}\frac{\hbar^2}{2\mathcal{J}}\langle\Lambda-2,n'|\gamma|\Lambda n\rangle\sqrt{I(I+1)-K(K-1)} \\
&\times\{\delta_{K',K-1}\delta_{\Lambda',\Lambda-2}[\delta_{\rho',\rho+1}\delta_{\sigma'\sigma}\delta_{\tau'\tau}(uu)^p_{\rho+1}+\delta_{\rho'\rho}\delta_{\sigma',\sigma+1}\delta_{\tau'\tau}(uu)^n_{\sigma+1}+\delta_{\rho'\rho}\delta_{\sigma'\sigma}\delta_{\tau',\tau+1}(uu)^n_{\tau+1}] \\
&\quad+(-1)^{I-j_p}\delta_{K'K}\delta_{K,1/2}\delta_{\Lambda',-\Lambda+2}[\delta_{\rho',-\rho-1}\delta_{\sigma',-\tau}\delta_{\tau',-\sigma}(uu)^p_{\rho+1}+\delta_{\rho',-\rho}\delta_{\sigma',-\tau}\delta_{\tau',-\sigma-1}(uu)^n_{\sigma+1} \\
&\qquad+\delta_{\rho',-\rho}\delta_{\sigma',-\tau-1}\delta_{\tau',-\sigma}(uu)^n_{\tau+1}]\} \\
&-\frac{2a_\gamma}{\sqrt{3}}\frac{\hbar^2}{2\mathcal{J}}\delta_{K'K}[\delta_{\Lambda',\Lambda-2}\langle\Lambda-2,n'|\gamma|\Lambda n\rangle \\
&\qquad\times(\delta_{\rho'\rho}\{\delta_{\sigma',\sigma+2}\delta_{\tau'\tau}[(uu)(uu)]^n_{\sigma+2}+(\delta_{\sigma'\sigma}\delta_{\tau',\tau+2}-\delta_{\sigma',\tau+2}\delta_{\tau'\sigma})[(uu)(uu)]^n_{\tau+2} \\
&\qquad\quad+\delta_{\sigma',\sigma+1}\delta_{\tau',\tau+1}(uu)^n_{\sigma+1}(uu)^n_{\tau+1}+\delta_{\sigma'+\tau',1}\delta_{\sigma+\tau,-1}(uv)^n_{\sigma'}(uv)^n_{\sigma+1}\} \\
&\qquad+\delta_{\rho',\rho+1}(uu)^p_{\rho+1}[\delta_{\sigma',\sigma+1}\delta_{\tau'\tau}(uu)^n_{\sigma+1}+\delta_{\sigma'\sigma}\delta_{\tau',\tau+1}(uu)^n_{\tau+1}] \\
&\qquad+\delta_{\rho',\rho+2}\delta_{\sigma'\sigma}\delta_{\tau'\tau}[(uu)(uu)]^p_{\rho+2}) \\
&\qquad+\delta_{\Lambda',\Lambda+2}\langle\Lambda+2,n'|\gamma|\Lambda n\rangle \\
&\qquad\times(\delta_{\rho'\rho}\{(\delta_{\sigma',\sigma-2}\delta_{\tau'\tau}-\delta_{\sigma'\tau}\delta_{\tau',\sigma-2})[(uu)(uu)]^n_\sigma+\delta_{\sigma'\sigma}\delta_{\tau',\tau-2}[(uu)(uu)]^n_\tau \\
&\qquad\quad+\delta_{\sigma',\sigma-1}\delta_{\tau',\tau-1}(uu)^n_\sigma(uu)^n_\tau+\delta_{\sigma'+\tau',-1}\delta_{\sigma+\tau,1}(uv)^n_{\sigma'+1}(uv)^n_\sigma\} \\
&\qquad+\delta_{\rho',\rho-1}(uu)^p_\rho[\delta_{\sigma',\sigma-1}\delta_{\tau'\tau}(uu)^n_\sigma+\delta_{\sigma'\sigma}\delta_{\tau',\tau-1}(uu)^n_\tau]+\delta_{\rho',\rho-2}\delta_{\sigma'\sigma}\delta_{\tau'\tau}[(uu)(uu)]^p_\rho)] \\
&+\frac{1}{\sqrt{2}}q_p\beta\delta_{K'K}\delta_{\sigma'\sigma}\delta_{\tau'\tau}(\delta_{\rho',\rho+2}\delta_{\Lambda',\Lambda-2}\langle\Lambda-2,n'|\gamma|\Lambda n\rangle\langle uu\rangle^p_{\rho+2}+\delta_{\rho',\rho-2}\delta_{\Lambda',\Lambda+2}\langle\Lambda+2,n'|\gamma|\Lambda n\rangle\langle uu\rangle^p_\rho) \\
&+\frac{1}{\sqrt{2}}q_n\beta\delta_{K'K}\delta_{\rho'\rho}\{\delta_{\Lambda',\Lambda-2}\langle\Lambda-2,n'|\gamma|\Lambda n\rangle[\delta_{\sigma',\sigma+2}\delta_{\tau'\tau}\langle uu\rangle^n_{\sigma+2}+(\delta_{\sigma'\sigma}\delta_{\tau',\tau+2}-\delta_{\sigma',\tau+2}\delta_{\tau'\sigma})\langle uu\rangle^n_{\tau+2}] \\
&\qquad+\delta_{\Lambda',\Lambda+2}\langle\Lambda+2,n'|\gamma|\Lambda n\rangle[(\delta_{\sigma',\sigma-2}\delta_{\tau'\tau}-\delta_{\sigma'\tau}\delta_{\tau',\sigma-2})\langle uu\rangle^n_\sigma+\delta_{\sigma'\sigma}\delta_{\tau',\tau-2}\langle uu\rangle^n_\tau]\} \\
&+\delta_{K'K}\delta_{\Lambda'\Lambda}\delta_{n'n}[\delta_{\tau'\tau}V_{pn}(\rho'\sigma';\rho\sigma)-\delta_{\sigma'\tau}V_{pn}(\rho'\tau';\rho\sigma)-\delta_{\tau'\sigma}V_{pn}(\rho'\sigma';\rho\tau)+\delta_{\sigma'\sigma}V_{pn}(\rho'\tau';\rho\tau)]\ . \qquad \text{(A13)}
\end{aligned}
$$

APPENDIX B: RELATION BETWEEN MOMENTS OF INERTIA AND PROPERTIES OF γ-VIBRATION

B_γ and C_γ appearing in Eq. (2.22) are related to E_γ and b^2 through Eqs. (2.25) and (2.27). Eliminating C_γ from these equations we obtain

$$B_\gamma = \frac{\hbar^2}{\beta^2 E_\gamma b^2} . \tag{B1}$$

On the other hand, Eq. (2.21) gives

$$B_\gamma = B'_\gamma(\gamma=0°) = B_0 - B_1 - B_2 . \tag{B2}$$

Equations (B1) and (B2) lead to

$$B_0 - B_1 - B_2 = \frac{\hbar^2}{\beta^2 E_\gamma b^2} . \tag{B3}$$

We can solve Eqs. (2.14), (2.16), and (B3) with respect to B_0, B_1, and B_2:

$$B_0 = \frac{\hbar^2}{3\beta^2}\left[\frac{1}{3}\frac{2\mathcal{J}}{\hbar^2} + \frac{1}{E_\gamma b^2}\right] , \tag{B4}$$

$$B_1 = \frac{4\hbar^2}{9\beta^2}\left[\frac{2-a_\gamma}{6}\frac{2\mathcal{J}}{\hbar^2} - \frac{1}{E_\gamma b^2}\right] , \tag{B5}$$

$$B_2 = \frac{2\hbar^2}{9\beta^2}\left[\frac{2a_\gamma - 1}{6}\frac{2\mathcal{J}}{\hbar^2} - \frac{1}{E_\gamma b^2}\right] . \tag{B6}$$

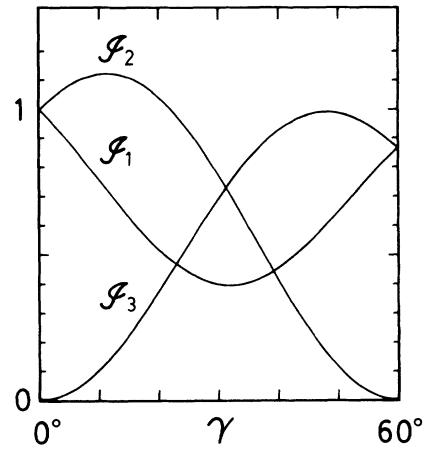

FIG. 12. The dependence on γ of the moments of inertia used for ^{157}Ho. The unit is $\mathcal{J}$ [see Eq. (2.14)]. Only their values and first derivatives at $\gamma=0°$ play roles in the present model.

The values of β, $\mathcal{J}$, E_γ, and b^2 used in the calculation for ^{157}Ho and $a_\gamma=-1$ give $B_0=149$, $B_1=12.8$, and $B_2=-121$ in units of $\hbar^2$/MeV. The moments of inertia corresponding to these B's are illustrated in Fig. 12. They are not symmetric under the $\gamma\rightarrow 60°-\gamma$ transformation, reflecting nonvanishing B_1 term.

*Present address: Shizuoka Institute of Science and Technology, 2174-1 Toyosawa, Fukuroi, Shizuoka 437, Japan.

[1]A. J. Larabee and J. C. Waddington, Phys. Rev. C **24**, 2367 (1981).

[2]R. Holzmann, J. Kuzminski, M. Loiselet, M. A. Van Hove, and J. Vervier, Phys. Rev. Lett. **50**, 1834 (1983).

[3]A. J. Larabee, L. H. Courtney, S. Frauendorf, L. L. Riedinger, J. C. Waddington, M. P. Fewell, N. R. Johnson, I. Y. Lee, and F. K. McGowan, Phys. Rev. C **29**, 1934 (1984).

[4]R. Holzmann, M. Loiselet, M. A. Van Hove, and J. Vervier, Phys. Rev. C **31**, 421 (1985).

[5]J. Simpson, B. M. Nyakó, A. R. Mokhtar, M. Bentley, H. W. Cranmer-Gordon, P. D. Forsyth, J. D. Morrison, J. F. Sharpey-Schafer, M. A. Riley, J. D. Garrett, C.-H. Yu, A. Johnson, J. Nyberg, and R. Wyss, in *Proceedings of the International Nuclear Physics Conference* (Harrogate, United Kingdom, 1986), Vol. 1, p. B66.

[6]J. Gascon, P. Taras, D. C. Radford, D. Ward, H. R. Andrews, and F. Banville, Nucl. Phys. **A467**, 539 (1987).

[7]G. B. Hagemann, J. D. Garrett, B. Herskind, J. Kownacki, B. M. Nyakó, P. J. Nolan, J. F. Sharpey-Schafer, and P. O. Tjøm, Nucl. Phys. **A424**, 365 (1984).

[8]G. B. Hagemann, J. D. Garrett, B. Herskind, G. Sletten, P. O. Tjøm, A. Henriquez, F. Ingebretsen, J. Rekstad, G. Løvhøiden, and T. F. Thorsteinsen, Phys. Rev. C **25**, 3224 (1982).

[9]J. Simpson, P. D. Forsyth, D. Howe, B. M. Nyakó, M. A. Riley, J. F. Sharpey-Schafer, J. Bacelar, J. D. Garrett, G. B. Hagemann, B. Herskind, A. Holm, and P. O. Tjøm, Phys. Rev. Lett. **54**, 1132 (1985).

[10]D. C. Radford, H. R. Andrews, D. Horn, D. Ward, F. Banville, S. Flibotte, P. Taras, J. Johanssen, D. Tucker, and J. C. Waddington, Workshop on Nuclear Structure, slide report, 16–20 May 1988, The Niels Bohr Institute, p. 124.

[11]G. B. Hagemann, J. Gascon, C.-H. Yu, D. C. Radford, and I. Hamamoto, XXIV Zakopane school, 1989, to be published.

[12]C.-H. Yu, M. A. Riley, J. D. Garrett, G. B. Hagemann, J. Simpson, P. D. Forsyth, A. R. Mokhtar, J. D. Morrison, B. M. Nyakó, J. F. Sharpey-Schafer, and R. Wyss, Nucl. Phys. **A489**, 477 (1988).

[13]K. Honkanen, H. C. Griffin, D. G. Sarantites, V. Abenante, L. A. Adler, C. Baktash, Y. S. Chen, O. Dietzsch, M. L. Halbert, D. C. Hensley, N. R. Johnson, A. J. Larabee, I. Y. Lee, L. L. Riedinger, J. X. Saladin, T. M. Semkow, and Y. Schutz, in *Nuclei Off the Line of Stability 1986,* edited by R. A. Meyer and D. S. Brenner (American Chemical Society Symposium Series No. 324), p. 555.

[14]P. J. Twin, P. J. Nolan, R. Aryaeinejad, D. J. G. Love, A. H. Nelson, and A. Kirwan, Nucl. Phys. **A409**, 343c (1983).

[15]S. Jónsson, J. Lyttkens, L. Carlén, N. Roy, H. Ryde, W. Waluś, J. Kownacki, G. B. Hagemann, B. Herskind, J. D. Garrett, and P. O. Tjøm, Nucl. Phys. **A422**, 397 (1984).

[16]P. Frandsen, J. D. Garrett, G. B. Hagemann, B. Herskind, M. A. Riley, R. Chapman, J. C. Lisle, J. N. Mo, L. Carlén, J. Lyttkens, H. Ryde, and P. M. Walker, Phys. Lett. B **177**, 287 (1986).

[17]P. Frandsen, R. Chapman, J. D. Garrett, G. B. Hagemann, B. Herskind, C.-H. Yu, K. Schiffer, D. Clarke, F. Khazaie, J. C. Lisle, J. N. Mo, L. Carlén, P. Ekström, and H. Ryde, Nucl. Phys. **A489**, 508 (1988).

[18]A. Ikeda and T. Shimano, Phys. Rev. Lett. **63**, 139 (1989).

[19]I. Hamamoto and B. R. Mottelson, Phys. Lett. **132B**, 7 (1983).

[20]A. Ikeda, Nucl. Phys. **A439**, 317 (1985).
[21]S. T. Belyaev, Nucl. Phys. **64**, 17 (1965).
[22]A. H. Wapstra and G. Audi, Nucl. Phys. **A432**, 1 (1985).
[23]S. Raman, C. H. Malarkey, W. T. Milner, C. W. Nestor, Jr., and P. H. Stelson, At. Data Nucl. Data Tables **36**, 1 (1987).
[24]M. Sakai, At. Data Nucl. Data Tables **31**, 399 (1984).
[25]R. G. Helmer, Nucl. Data Sheets **52**, 1 (1987).
[26]R. G. Helmer, Nucl. Data Sheets **49**, 383 (1986).
[27]M. A. Lee, Nucl. Data Sheets **56**, 199 (1989).
[28]M. A. Lee and R. L. Bunting, Nucl. Data Sheets **46**, 187 (1985).
[29]A. E. Ignatochkin, E. N. Shurshikov, and Y. F. Jaborov, Nucl. Data Sheets **52**, 365 (1987).
[30]Aa. Bohr and B. R. Mottelson, *Nuclear Structure* (Benjamin, New York, 1975), Vol. II, pp. 509 and 512.